Solar-powered smart textiles, electronic textiles, and wearable electronics

Mohammad Hatamvand[a], Ehsan Kamrani[b,c], Mónica Lira-Cantú[d], Morten Madsen[e], Paola Vivo[f], Yiqiang Zhan[a,*]

[a] Center of Micro-Nano System, Fudan University, Shanghai 200433, China
[b] Center for Intelligent Antenna and Radio System (CIARS), Department of Electrical & Computer Engineering, University of Waterloo, Waterloo, ON, Canada
[c] Wellman Center for Photomedicine, Harvard Medical School, Boston, MA, USA
[d] Catalan Institute of Nanoscience and Nanotechnology (ICN2), CSIC and The Barcelona Institute of Science and Technology, Campus UAB, Bellaterra E-08193, Barcelona, Spain
[e] SDU NanoSYD, Mads Clausen Institute, University of Southern Denmark, Alsion 2, 6400 Sønderborg, Denmark
[f] Faculty of Engineering and Natural Sciences, Tampere University, P.O. Box 541, FI-33101 Tampere, Finland

∗ Corresponding author.

*E-mail address: yqzhan@fudan.edu.cn

Abstract

During the last few years, textile solar cells with planar and fiber-shaped configurations have attracted enormous research interest. These flexible-type solar cells have a huge potential applicability in self-powered and battery-less electronics, which will impact many sectors, and particularly Internet of Things. Textile solar cells are lightweight, super-flexible, formable, and foldable. Thus, they could be ideal power-harvester alternatives to common flexible solar cells required in smart textiles, electronic textiles, and wearable electronic devices. This review presents a brief overview to fiber-shaped and planar-shaped solar cells, and it introduces the most recent research reports on the different types of textile solar cells, including their fabrication techniques. Finally, their current challenges and limitations with respect to their fabrication methods, and the issues encounter for their implementation and integration in novel devices, are also described.

Keywords: Fiber-shaped solar cells, Textile solar cells, planar-shaped solar cells; Flexible solar cells, Photovoltaic textiles, power harvesting, smart textiles, electronic textiles, wearable electronic devices

1. Introduction

The use of fossil fuels for supplying the worldwide growing energy demand is one of the most important human concerns, as these energy sources lead to environmental pollution due to the release of carbon dioxide and other greenhouse gases. This results in global warming and climate changes, which is a significant challenge in a world with a still rapid growing population. Thus, the utilization of clean and renewable energy resources is an urgent and high-demand necessity. Solar energy is a promising alternative to fossil fuels, since it is renewable, clean, eco-friendly, sustainable, abundant, and readily available. Hence, many research efforts have been invested on improving the performance, efficiency and stability of different types of emerging photovoltaics (PVs) such as dye sensitized,[1–10] organic,[11–22] and perovskite PVs.[23–42] While conventional silicon solar cells are heavy, fragile, and rigid, flexible solar cells represent a good alternative to the silicon counterparts, because of not only their flexibility, but also their lightweight, which enable their integration in portable electronic applications. Recently, scientists have carried out significant research and development efforts in order to improve the performance and the stability of flexible solar cells.[43–61] Their photoactive materials should be able to generate high power conversion efficiencies (PCE) while having at the same time excellent tolerance towards mechanical bending and

stretching stress.[62] However, despite the progress of the latest years, flexible solar cells can still only endure a limited bending radius, ultimately limiting their applicability in flexible products, such as cases where formability, pliability, foldability, and wearability are requested.

The convergence and integration of textiles and electronics result in smart textiles and electronic textiles (e-textiles), which are able to sense, react or adapt to the environment. The textile industry is experiencing a growing demand for high-tech materials with the increasing integration of e-textiles to create self-powered wearable electronic devices (WEDs). Due to their unique formable structure, WEDs are promising to be used in various fields such as health care, sport or military applications.[63,64,65]

Textile solar cells can be fabricated in two ways, namely from 1) fiber-shaped solar cells (FSSCs) that are interlaced together, or 2) planar-shaped solar cells (PSSCs) that are fabricated directly on a textile substrate. In contrast to PSSCs that could absorb light only from one side, FSSCs could potentially harvest sunlight from all three dimensions due to their cylindrical structure.[66] In addition, as they are light-weight and compatible with fabric weaving, their integration into textiles can be utilized for various applications.[67] PSSCs have also another advantage with respect to FSSCs, which is their easier processing via direct fabrication on a prepared textile substrate.

In this review, we present an overview of textile solar cells, made from FSSCs or PSSCs, as a new generation of flexible solar cells. FSSCs and PSSCs could potentially play significant role in future applications, and especially for the development of battery-less self-powered electronics for wearables and the Internet of Things (IoT). Although self-powered wearable smart textiles and e-textiles need to simultaneously harvest and store the required electrical energy, [68] the focus of this review is limited to the research progress made on various types of power-harvesting textile solar cells in the latest years (and not to their integration in devices). We highlight their relevant fabrication techniques, their advantages and limitations together with their current challenges to be overcome in the next years. Finally, the perspectives of FSSCs and PSSCs research are discussed.

2. Structure and performance of flexible FSSCs

In order to fabricate a FSSC, the PV active layers should be coated on a cylindrical substrate (e.g. thread, metal or carbon wire, optical fiber, among others). Their functioning takes place by either absorbing the light from the external coated layer, or, in the case of an optical fiber, by in-coupling of light from the cross section of the fiber into internal PV active layers.[69] The fabricated FSSCs can subsequently be embedded inside a textile or interlaced together in order to form a textile solar cell. Recent research and development efforts have led to fabrication of fiber-shaped dye-sensitized solar cells (FSDSSCs),[70–84] fiber-shaped organic solar cells (FSOSCs),[85–88] and fiber-shaped perovskite solar cells (FSPSCs).[89–97] Figure 1 shows a schematic drawing for some of the fabricated FSSCs demonstrated to date. Their structure and PV parameters, including short-circuit current density (J_{SC}), open-circuit voltage (V_{OC}), fill factor (FF) and power conversion efficiency (PCE), are also summarized in Table 1. For these FSSCs, the structure, fabrication techniques, performance, and applications have been well studied and reported.[98–100]
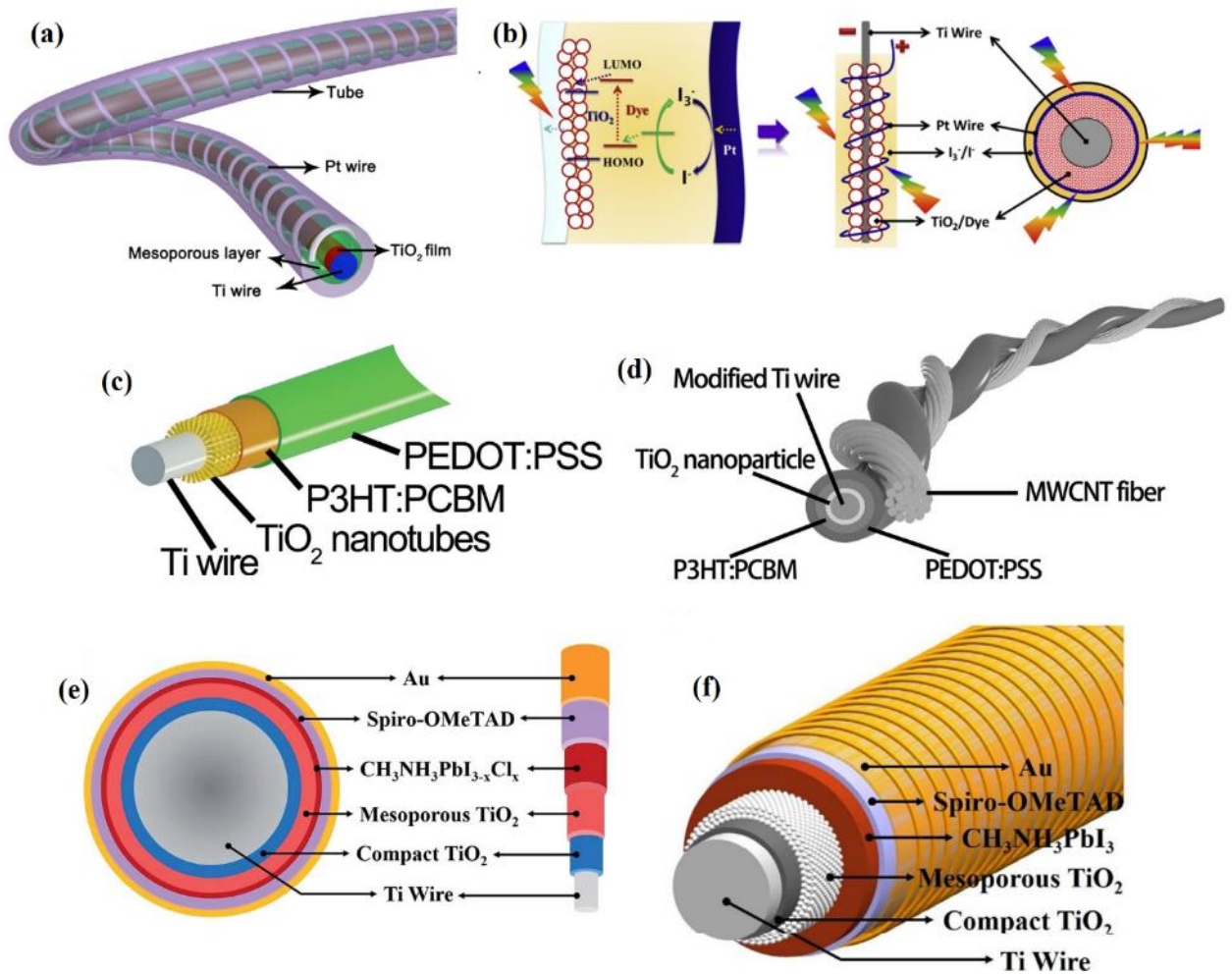
Figure 1. Schematic representation of a) FSDSSC[79] b) FSDSSC from different views showing the PV mechanism[73] c) FSOSC[85] d) FSOSC with multi walled carbon nano tube (MWCNT) as the top electrode[88] e) top vie and cross section of a FSPSC[93] and f) FSPSC with different coated PV layers.[97]

Table 1. Structure and PV parameters of different types of fabricated FSCs

Structure	Type	J_{SC} (mA cm^{-2})	V_{OC} (V)	FF	PCE (%)	Ref
Ti wire / TiO$_2$ NPL / N719 / I$^-$-I$_3^-$ / Pt wire	DSSC	10.60	0.68	0.83	6.00	[70]
Ti wire / TiO$_2$ CL / TiO$_2$ NPL / N719 / I$^-$-I$_3^-$ / Pt wire	DSSC	12.58	0.68	0.71	6.12	[83]
Ti wire / graphene-TiO$_2$ / N719 / I$^-$-I$_3^-$ / Pt wire	DSSC	6.09	0.75	0.70	3.26	[82]
Ti wire / aligned TiO2 nanotube arrays / N719 / I$^-$-I$_3^-$ / MWCNT array	DSSC	16	0.71	0.61	7.13	[76]
Ti wire / TiO$_2$ NPs / organic dye / I$^-$-I$_3^-$ / Pt wire	DSSC	7.54	0.64	0.64	3.12	[73]
Ti wire / TiO$_2$ nanotube / N719 / I$^-$-I$_3^-$ / Pt-coated carbon fiber	DSSC	11.92	0.74	0.64	5.64	[80]
Ti wire / TiO$_2$ nanotube arrays / N719 / I$^-$-I$_3^-$ / CoNi$_2$S$_4$ nanoribbon-CF	DSSC	15.30	0.68	0.68	7.03	[78]
Ti wire / TiO$_2$ nanotube arrays / N719 / I$^-$-I$_3^-$ / CoNi$_2$S$_4$ nanorod-CF	DSSC	8.60	0.65	0.73	4.10	[78]
Ti wire / TiO$_2$ nanotube arrays / N719 / I$^-$-I$_3^-$ / Pt wire	DSSC	14.20	0.68	0.67	6.45	[78]
Ti wire / TiO$_2$ nanotube arrays / N719 / I$^-$-I$_3^-$ / Bare CF	DSSC	7.10	0.65	0.23	1.03	[78]
spring-like Ti wire / TiO$_2$ nanowire array / N719 / I$^-$-I$_3^-$ / Pt wire	DSSC	7.58	0.69	0.60	3.13	[81]
Ti wire/ TiO$_2$ NPs / N719 / I$^-$-I$_3^-$ / Pt wire	DSSC	10.36	0.63	0.71	5.03	[71]
Ti wire with Microridges / TiO$_2$ NPs / N719 / I$^-$-I$_3^-$ / Pt wire	DSSC	12.34	0.69	0.74	6.29	[71]
Ti wire with microridges : nano rods / TiO$_2$ NPs / N719 / I$^-$-I$_3^-$ / Pt wire	DSSC	14.79	0.70	0.78	8.13	[71]
Ti wire with Ti nanorods / TiO$_2$ NPs / N719 / I$^-$-I$_3^-$ / Pt wire	DSSC	13.10	0.70	0.77	7.05	[71]
Ti wire/ TiO2 nanotube array / N719 / I$^-$-I$_3^-$ / Pt:CS-CNT composite fiber	DSSC	19.43	0.73	0.71	10.00	[84]
Ti wire / aligned titania nanotubes / N719 / I$^-$-I$_3^-$ / Aligned CNT fibers	DSSC	8.60	0.68	0.38	2.20	[72]
Ti wire / aligned titania nanotubes / TiO$_2$ NPs / P3HT:PCBM / PEDOT:PSS / aligned MWCNT fiber	OPV	7.38	0.53	0.41	1.60	[88]
Ti wire / aligned titania nanotubes / P3HT:PCBM / PEDOT:PSS / MWCNT sheet	OPV	6.33	0.51	0.38	1.23	[85]
CNT array / compact n-TiO$_2$ / meso-TiO$_2$ / CH 3 NH 3 PbI 3− x Cl x / P3HT:SWNT / Ag nanowire network / CNT array	OPV	8.75	0.62	0.56	3.03	[91]
Stainless steel wire / compact n-TiO$_2$ / meso-TiO$_2$ / MAPbI$_3$ / OMeTAD / CNT sheet	Perovskite	10.20	0.66	0.49	3.30	[89]
Ti wire / TiO$_2$ nanotube array / CH$_3$NH$_3$PbI$_3$ / CNT film	Perovskite	2.62	0.92	0.48	1.16	[96]
Ti wire / compact -TiO$_2$ / meso-TiO$_2$ / CH$_3$NH$_3$PbI$_3$ / Spiro-OMeTAD / Ag NWs	Perovskite	11.97	0.73	0.44	3.85	[90]
Ti wire / compact -TiO$_2$ / TiO$_2$ nanotube array / CH3NH3PbI3 / aligned CNT sheet	Perovskite	8.90	0.85	0.48	3.6	[94]
Ti wire / compact -TiO$_2$ / meso-TiO$_2$ / CH$_3$NH$_3$PbI$_3$ / Spiro-OMeTAD / Au	Perovskite	14.18	0.87	0.61	7.53	[97]
Ti wire / compact -TiO$_2$ / meso-TiO$_2$ / CH$_3$NH$_3$PbI$_{3-x}$Cl$_x$ / Spiro-OMeTAD / Au	Perovskite	12.32	0.71	0.61	5.35	[93]
(PEN/ITO) strip / compact -TiO$_2$ / CH$_3$NH$_3$PbI$_3$ / CNT sheet	Perovskite	15.90	0.91	0.66	9.49	[101]

3. Design and fabrication of textile-based PSSCs

3.1. Textile-based dye-sensitized PSSCs (PSDSSCs)
3.1.1. Counter electrodes in PSDSSCs

In 2014 Jie et al.[102] designed and fabricated a cotton textile counter electrode for a PSDSSC, in order to replace FTO in the cells. The electrode was coated with Ni by a low temperature electroless plating technique, and was prepared with polypyrrole (PPy) as a catalytic material by dip coating followed by in situ polymerization of the pyrrole monomer on the Ni-coated textile. Figure 2 shows the J-V characteristics of the fabricated PSDSSCs with the Pt-coated FTO and the PPy/Ni-coated fabric counter electrode. Testing of the adhesion between the Ni-coated electrode and fabric demonstrated relatively high resilience to delamination effects. As shown in Table 2, the PCE, fill factor, J_{sc}, and V_{oc} of the fabricated PSDSSC with the textile based counter electrode are all lower than the conventional DSSC with Pt-coated FTO counter electrode, dropping almost 50% in PCE when moving to a fabric electrode material. Still, this work is relevant because it demonstrated a possible route for development of a textile-based counter electrodes for PSDSSCs.
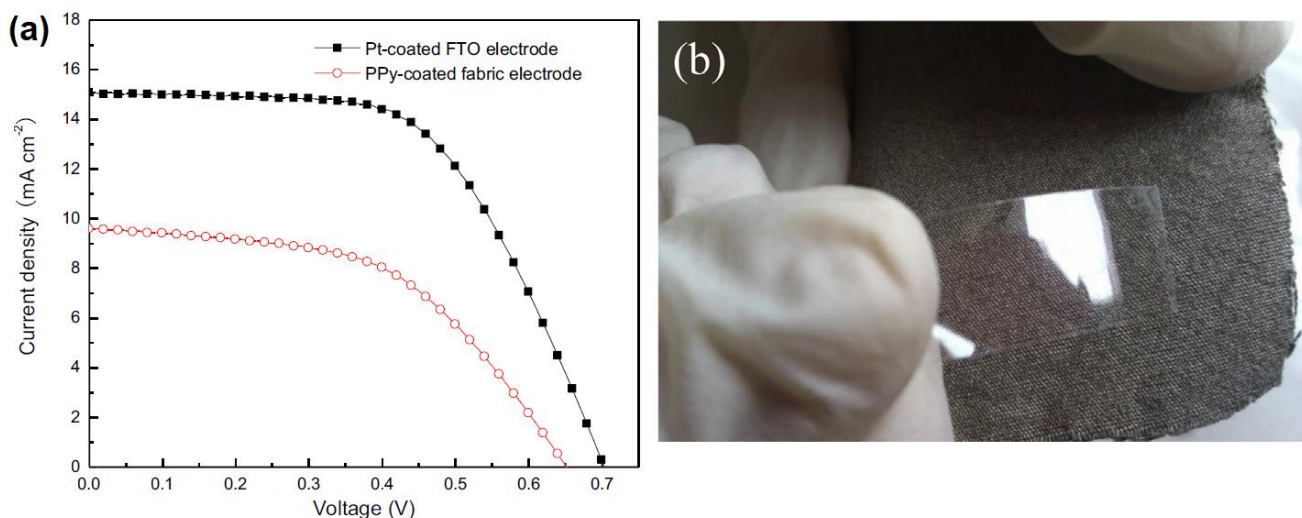

Figure 2. a) (J-V) characteristics of fabricated PSDSSCs with Pt-coated FTO and PPy/Ni-coated fabric counter electrodes measured under AM 1.5 illumination. b) testing the adhesion between Ni-coated and the fabric by tape paste.[102]

Table 2. PV parameters for both fabricated PSDSSCs with Pt-coated FTO and PPy/Ni-coated fabric counter electrodes.[102]

Counter electrode	J_{SC} (mA cm^{-2})	V_{OC} (mV)	FF	PCE (%)
Pt-coated FTO	15.10	704	0.58	6.16
PPY/Ni-Coted fabric	9.60	652	0.52	3.30

Alvira Ayoub Arbab et al.[103] fabricated another textile counter electrode with polyester fabrics in 2015. They demonstrated coating of a layer of multiwalled carbon nanotubes (MWCNT) with different thicknesses, and various different MWCNT sizes. Interestingly, different enzymes were used on the polyester fabric, via a simple tape casting technique, in order to decrease the agglomeration of the MWCNTs without perturbing their electronic properties. Figure 3 depicts the relevant different fabrication steps and the schematic illustration of different layers in the fabricated PSDSSC. Figure 4 also shows that the adhesion between the coated MWCNTs and fabric was strong, as proven by a scotch tape test. The device results, Figure 5 and Table 3, showed that, although the efficiency of the fabricated PSDSSC with the textile counter electrodes was lower than for the reference PSDSSC

with the standard pt-FTO coated glass counter electrodes, the PSDSSC with the flexible counter electrode demonstrate quite decent PCE values of 5.7%, due to an almost fully maintained V_{OC} and FF.
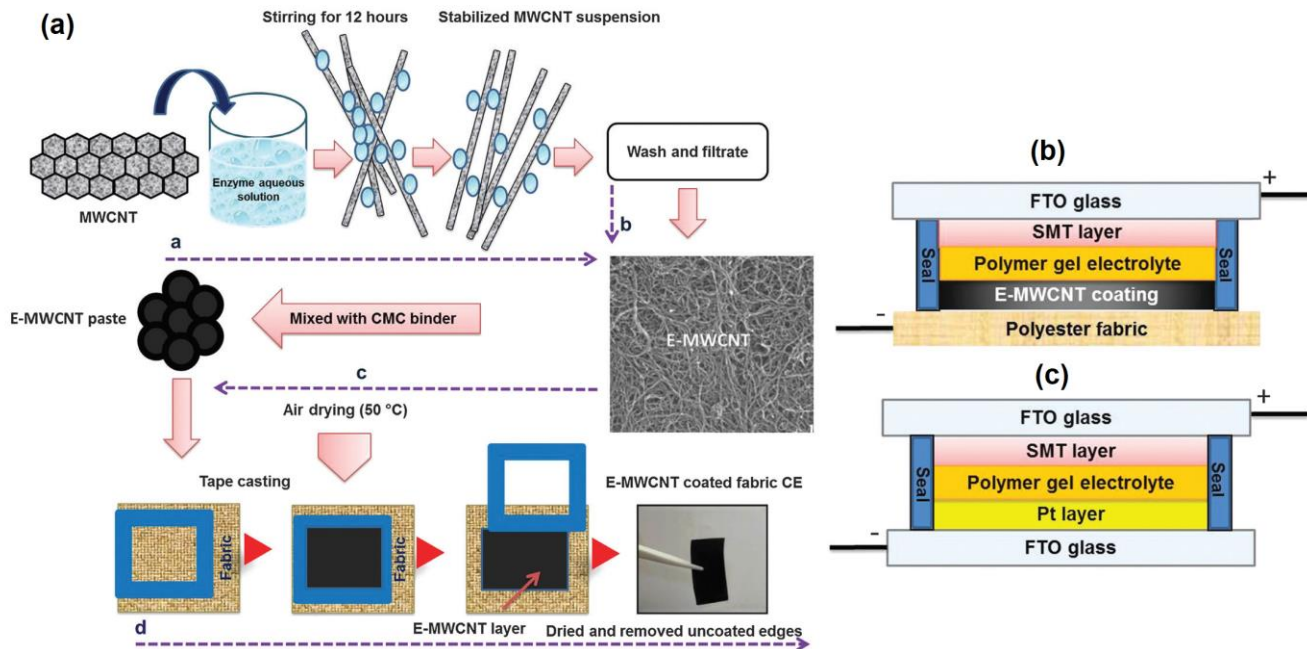

Figure 3. a) schematic illustration of different steps for fabrication of the PSDSSC with textile-based counter electrode b) schematic structure of PSDSSC with textile-based counter electrode c) schematic structure of conventional PSDSSC with Pt-coated FTO counter electrode.[103]
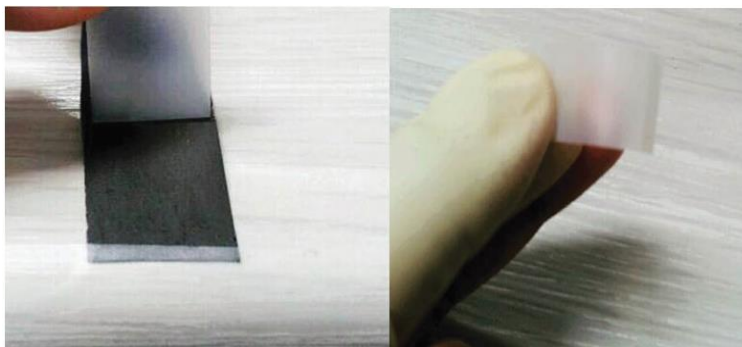

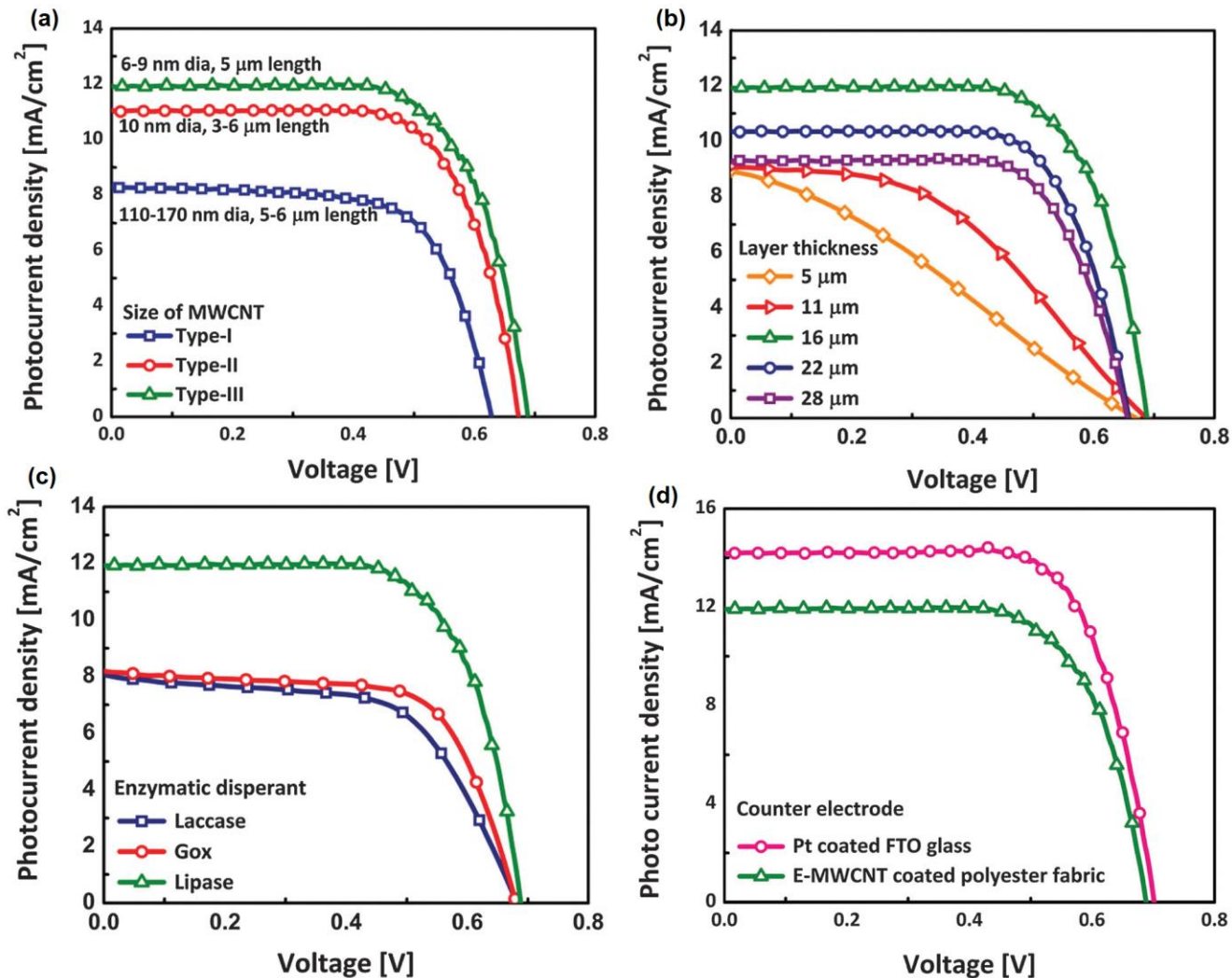Figure 4. Testing of the adhesion between the fabric and MWCNT layer.[103]

Figure 5. J-V characteristics of the fabricated PSDSSCs using a) different size of MWCNT b) different layer thickness of E-MWCNT c) different enzymes and d) the comparison between the conventional Pt coated FTO glass and the textile MWCNT coted counter electrodes.[103]

Table 3. PV parameters of fabricated PSDSSCs with different counter electrodes.[103]

Counter electrode	J_{SC} (mA cm^{-2})	V_{OC} (mV)	FF	PCE (%)
Pt/ FTO	14.18	701	0.72	7.16
E-MWCNT/ fabric	11.92	688	0.69	5.69

In a similar research work, Iftikhar Ali Sahito et al.[104] fabricated a flexible and highly conductive graphene-coated cotton fabric (HC-GCF), and employed it as a counter electrode in PSDSSCs. The graphene oxide nanosheets were coated by cationization of a cotton fabric, in order to develop a positively charged surface, followed by soaking of the cotton fabric in graphene oxide nanosheet (GON) dispersions. A chemical reduction method was used to turn the graphene oxide into graphene nanosheets, using a hydrazine monohydrate solution. The surface

resistance of the highly conductive graphene coated cotton fabric was 7 Ω sq^{-1}. A power conversion efficiency (PCE) of 6.93% was obtained in comparison to 8.44% for the DSSC with Pt-FTO counter electrodes. The fabrication process and device performance results are shown in Figure 6 and Table 4.
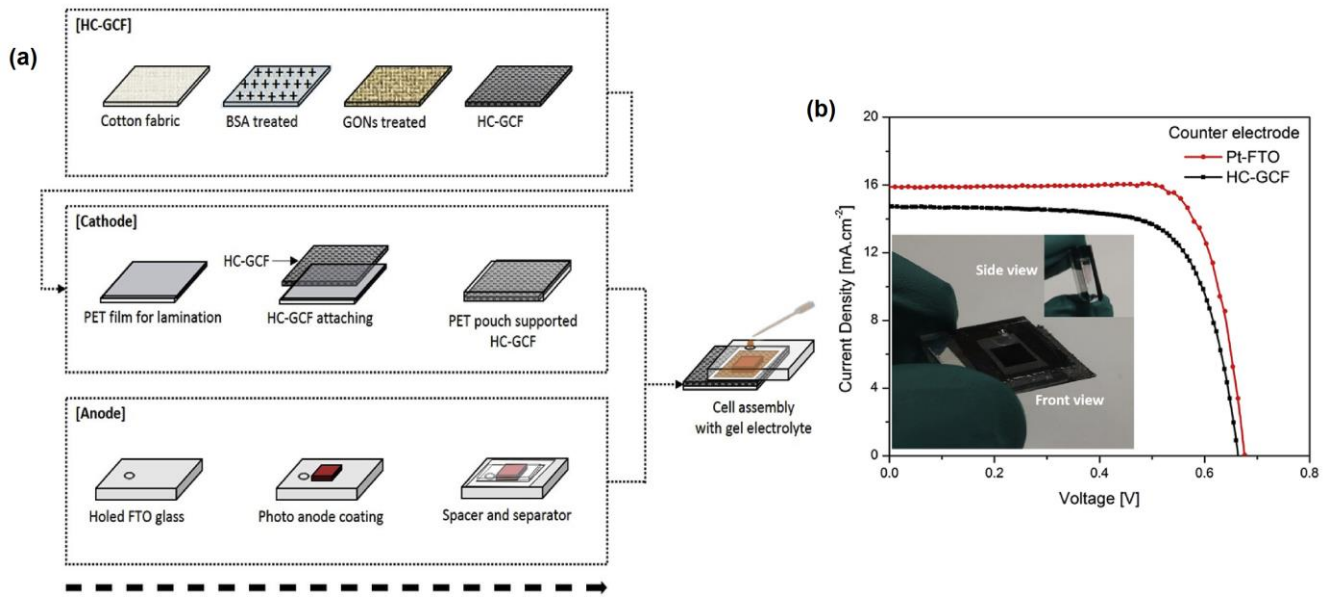

Figure 6. a) Schematic explanation of the different fabrication steps used for developing the PSDSSC with textile-based counter electrodes b) J-V curves of Pt and HC-GCF counter electrode based PSDSSCs.[104]

Table 4. PV characteristic of the Pt and HC-GCF counter electrode based PSDSSCs.[104]

Counter electrode	J_{SC} (mA cm^{-2})	V_{OC} (mV)	FF	PCE (%)
Pt - FTO	15.88	670	0.79	8.44
HC-CGF	14.75	660	0.71	6.93

In 2016 Alvira Ayoub Arbab et al.[105] fabricated a textile fabric counter electrode in PSDSSCs based on activated charcoal doped multi walled carbon nanotubes (AC doped MWCNT), which was printed on a 100% polyester woven fabric by doctor blading technique (Figure 7). Three types of activated charcoal coal (composite A), coconut shell (composite B) and pine tree (composite C) were used with different wt% of AC in order to fabricate the AC doped MWCNT. Results showed that the pine tree composite (composite C) with 0.8 wt% of AC into the MWCNT dispersions reached the highest PCE (7.29%) for the textile fabric counter electrodes (figure 8, tables 5-6). Figur 9 and table 7 depict the comparision between PV parameters of PSDSSCs fabricated with Pt and carbon fabric counter electrodes.
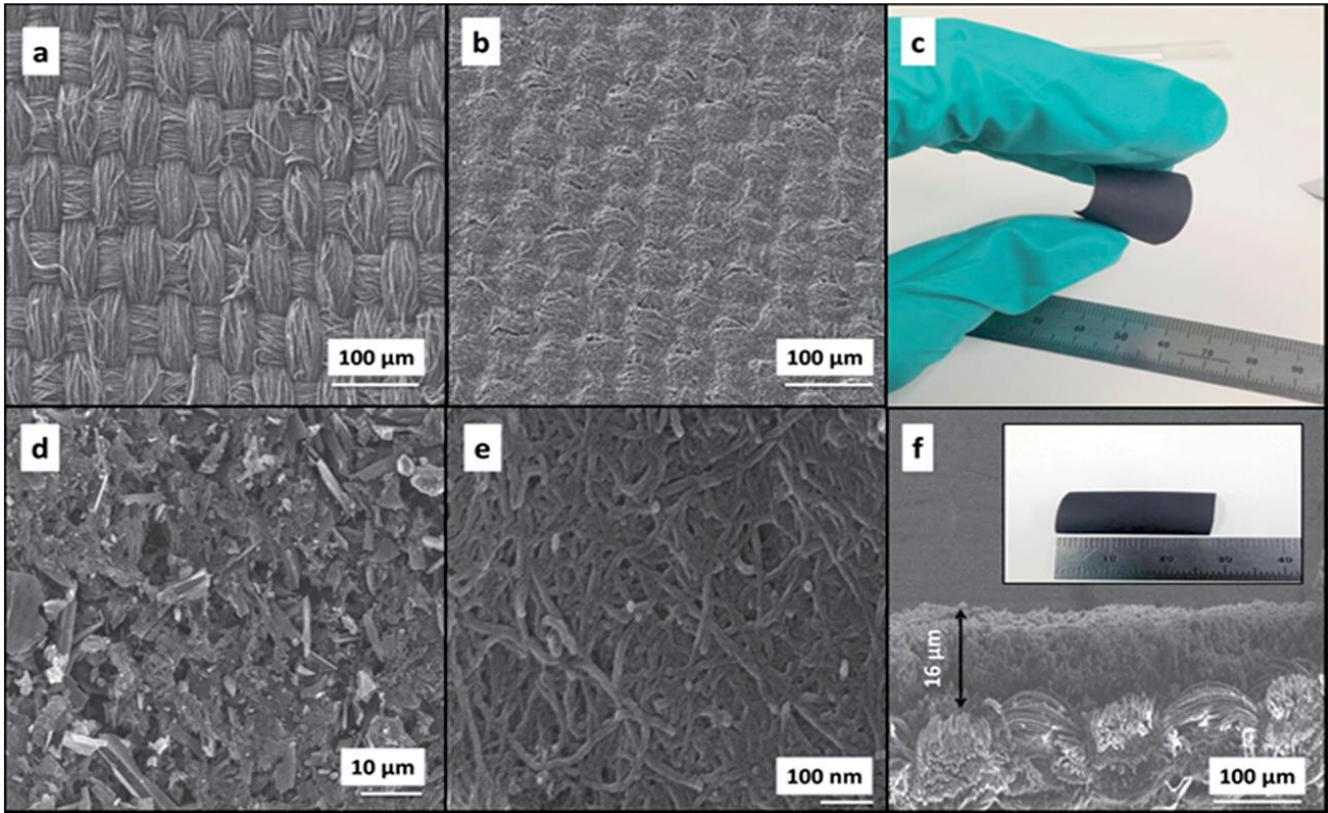
Figure 7. FE-SEM images of a) uncoated polyester fabric b) AC doped MWCNT coated fabric. c) image of the flexible carbon fabric d) Low magnification FE-SEM image of the AC doped MWCNT e) High magnification FE-SEM image of the AC doped MWCNT f) Cross-sectional FE-SEM image of the carbon fabric composite with the image of the carbon fabric composite.[105]
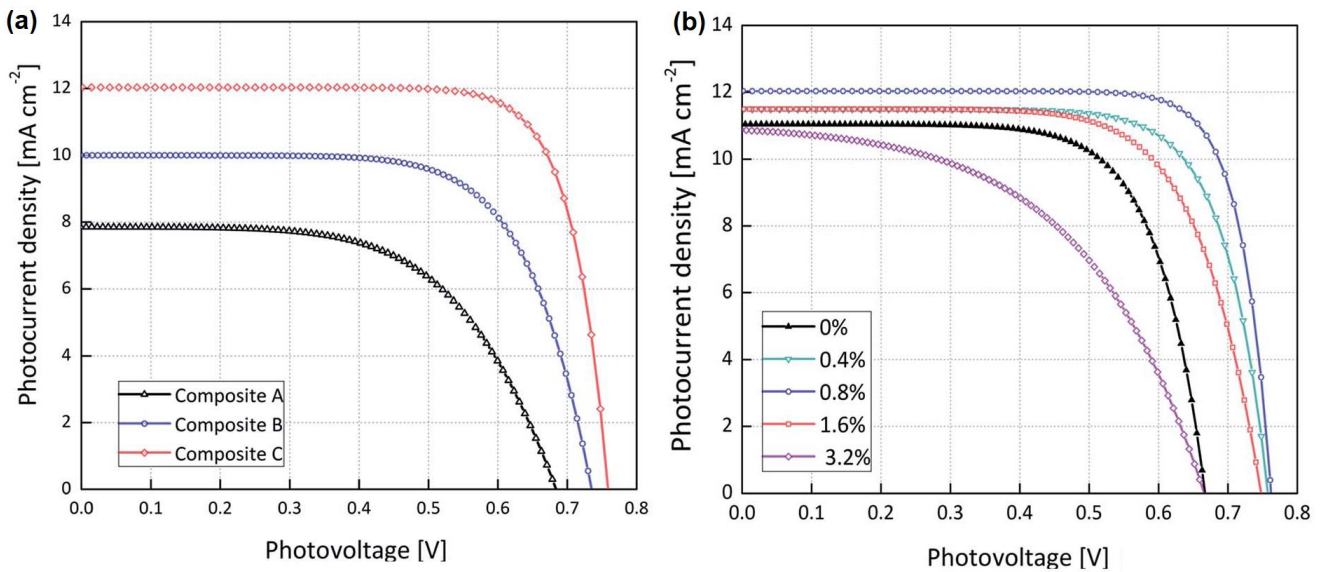
Figure 8. J-V curves of fabricated PSDSSCs based on a) three types (composite A, B and C) of carbon fabric composites counter electrodes and b) different wt% of charcoal on PV performance.[105]

Table 5. PV performance of PSDSSCs fabricated with different carbon fabric composites.[105]

Type of composite	J_{SC} (mA cm^{-2})	V_{OC} (mV)	FF	PCE (%)
Composite A	8.06	681	0.60	3.31
Composite B	10.09	735	0.68	5.03
Composite C	11.50	743	0.70	5.97

Table 6. PV performance of PSDSSCs fabricated with carbon fabric composites of different wt% of activated carbon (pine type).[105]

wt% of carbon	J_{SC} (mA cm^{-2})	V_{OC} (mV)	FF	PCE (%)
0	11.05	673	0.70	5.24
0.4	11.52	769	0.74	6.56
0.8	12.03	766	0.79	7.29
1.6	11.50	743	0.70	5.97
3.2	11.03	665	0.49	3.61

Table 7. The comparison between PV parameters of PSDSSCs fabricated with Pt and carbon fabric CEs.[105]

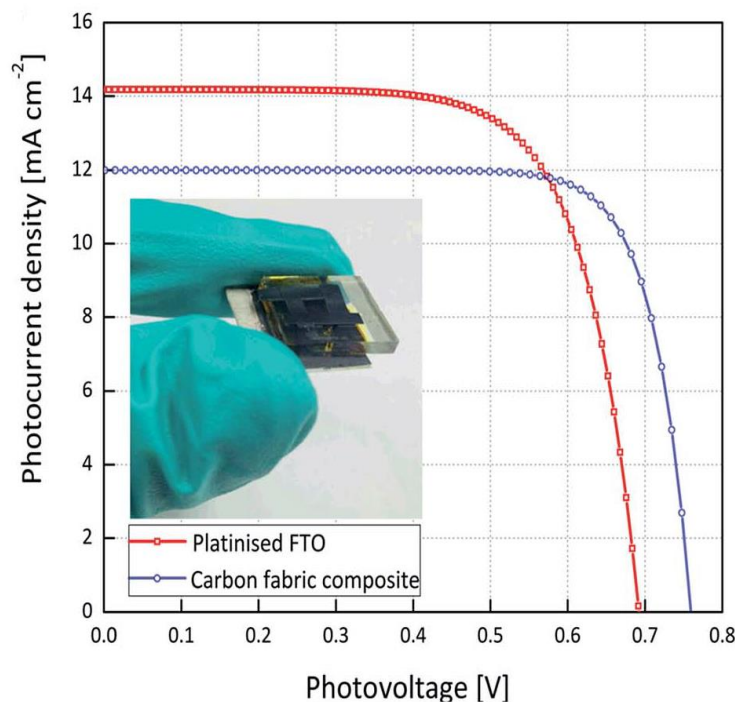| wt% of carbon	J_{SC} (mA cm^{-2})	V_{OC} (mV)	FF	PCE (%)
0	11.05	673	0.70	5.24
0.4	11.52	769	0.74	6.56

Figure 9. The comparison between I-V curves of PSDSSCs fabricated with Pt and carbon fabric CEs.[105]

Anam Ali Memon et al.[106] fabricated textile-based counter electrodes from cotton, polyester, and linen fibers using highly photo- and electro-catalytic activated carbon composites made from highly conductive functionalized multi-walled carbon nanotubes with mesoporous activated charcoal (M-AC/CNT). The power conversion efficiency of the fabricated PSDSSCs with the textile based counter electrodes based on polyester, cotton and linen was 6.26%, 6.06% and 5.80% respectively, which is comparable to the 7.26% delivered by the Pt-coated counter electrode reference.

3.1.2. Insertion of DSSCs into textiles

Min Ju Yun et al.[107] introduced in 2015 a new approach for the incorporation of DSSC electrodes into textiles during the weaving process of making the textile. In this structure, the TiO_2 dye-loaded porous was coated on a metal ribbon, which was used as the photoanode. Pt nanoparticle-loaded carbon yarn was used as the counter electrode. The photoanode and counter electrode was weaved together as the warp or weft. Finally, the fabricated DSSC textile solar cell was sewn into a garment. As shown in Figure 10, the Pt loaded carbon yarn was weaved as a weft, the counter electrode and the dye loaded TiO_2 on a stainless steel ribbon having the photoanode were weaved as warps in the bottom and top of the fabric, Nylon filaments were weaved as warps in order to support the photoanode metal ribbon and maintaining the space between the photoanode and the counter electrode for preventing short circuits until filling the electrolyte. Figure 10 shows the inserted DSSC inside a textile structure in details. The conversion efficiency of the inserted DSSC in the textile was 2.63%, having a J_{sc} of 5.78 mA/cm^{-2}, a V_{oc} of 0.725 V, and a fill factor of 0.63 (Figure 11).
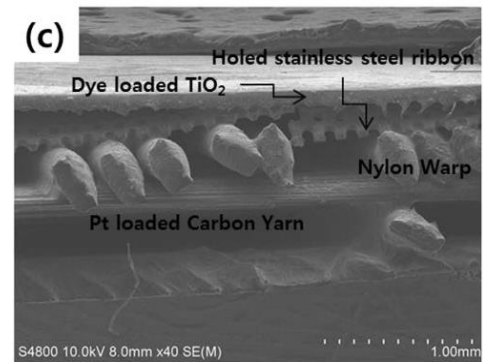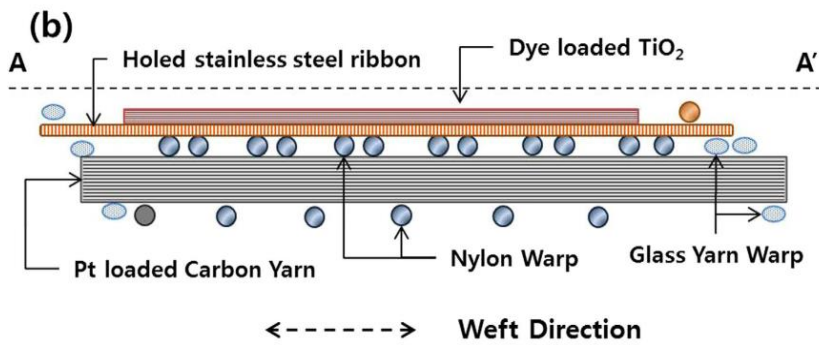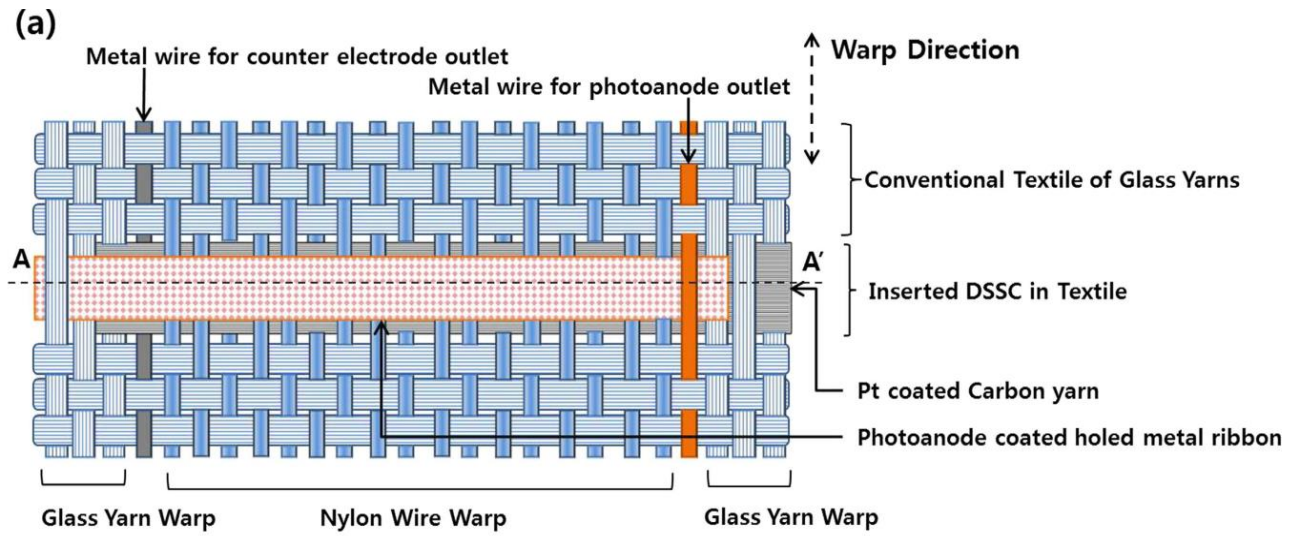
Figure 10. schematic illustration of the structure of the inserted DSSC into the textile from the a) top view b) cross section view and c) cross sectional SEM image.[107]
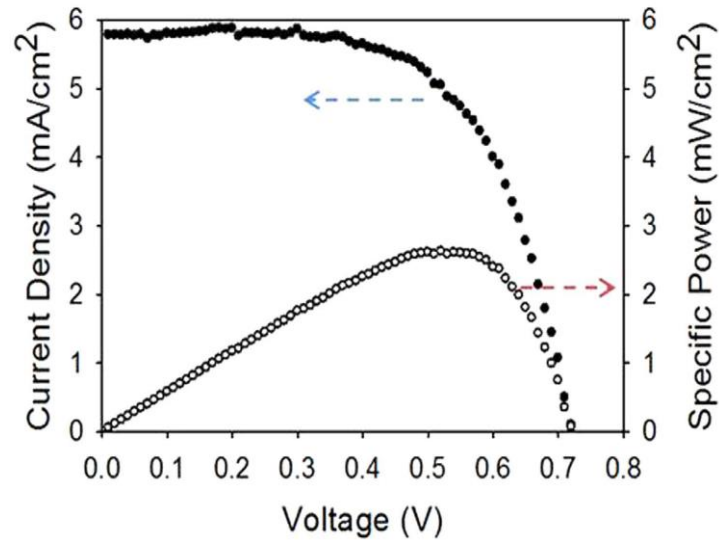

Figure 11. PV characteristics curves of inserted DSSC into the textile.[107]

Although this presents an innovative idea for weaving of DSSC devices into a textile structure, the fabricated textile solar cell was not still completely flexible due to inserting the metal ribbon and metal wires as different parts of the DSSC.

3.1.3. Coating DSSC layers on a textile

Klaus Opwis et al.[108] fabricated a textile-based PSDSSC on a woven fabric from glass-fibers. At first, they covered a glass-fiber fabric with a thin polyamide (PA) film made from roll-to-roll processing, in order to prepare a uniform and smooth surface for coating of the PV layers (Figure 12). Afterwards, a titanium layer was made by electron beam or sputter deposition, followed by screen printing of titanium dioxide and curing at 500°C for 5 min. The active layer was synthesized by ruthenium-based dyestuffs. After adding the electrolyte, a thin film of PEN + ITO was coated by the catalyst layer of Pt from the chemical reduction of H_2PtCl_6 at room temperature, which was used as the counter electrode on the previous layers. Finally, the fabricated PSDSSC (glass-fiber fabric + PA layer + Ti + dye-sensitized TiO_2 + electrolyte + PEN + ITO + Pt) was sealed by special epoxy thermoplastic foils (Figure 13). The best fabricated textile-based PSDSSC worked with 1.83% efficiency (Figure 14, Table 8). Although a novel and innovative prototype of a textile-based PSDSSC was fabricated via this approach, it was carried out on a woven glass-fiber that is more expensive than conventional woven fabrics. The fabrication process was also done at high temperatures (500 ℃), which finally unavoidably increases the fabrication costs. However, such development also puts emphasis on the need for smooth and uniform planarization layers, which yielded decent performance results in this work.
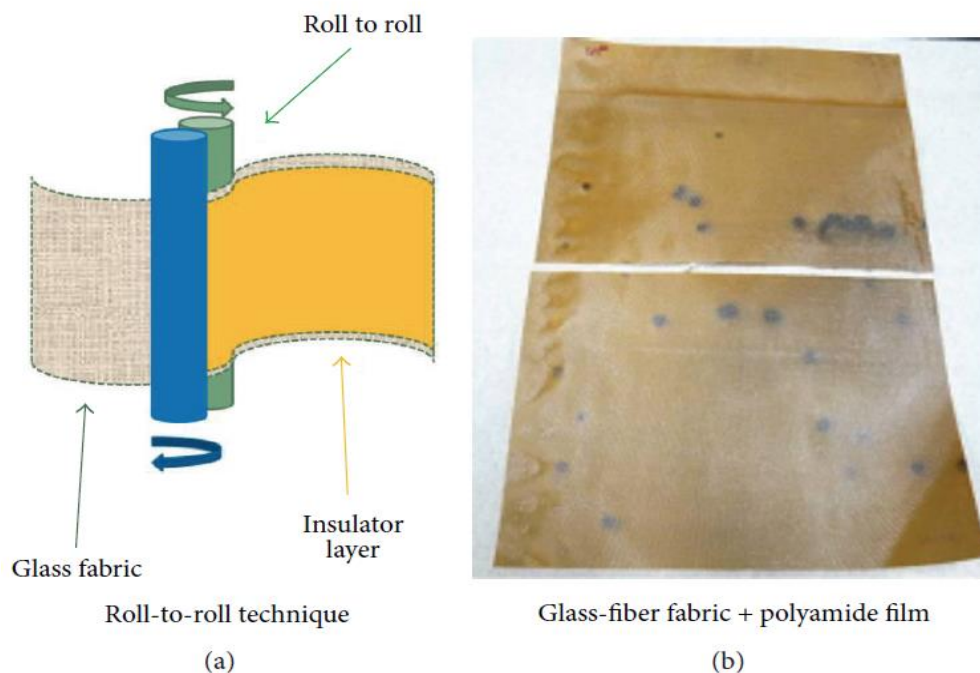
Figure 12. a) Schematic illustration of roll-to-roll coating technique b) The image of coated glass fiber fabric by PA.[108]

(a)   (b)
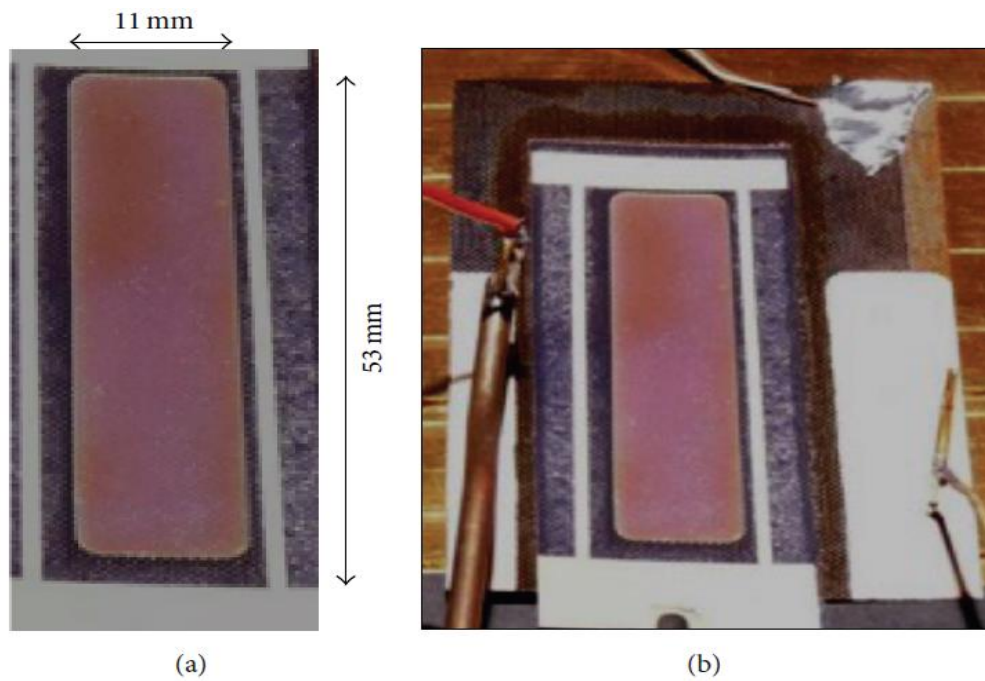
Figure 13. The images of a) prepared textile based PSDSSC b) 4-point configuration used for J-V characterization.[108]

Table 8. PV parameters of fabricated textile based PSDSSC at different irradiance level.[108]

Irradiance (W/m^2)	J_{SC} (mA cm^{-2})	V_{OC} (mV)	FF	PCE (%)
1000	5.10	790	0.27	1.10
500	2.55	750	0.39	1.51
200	0.95	710	0.54	1.83
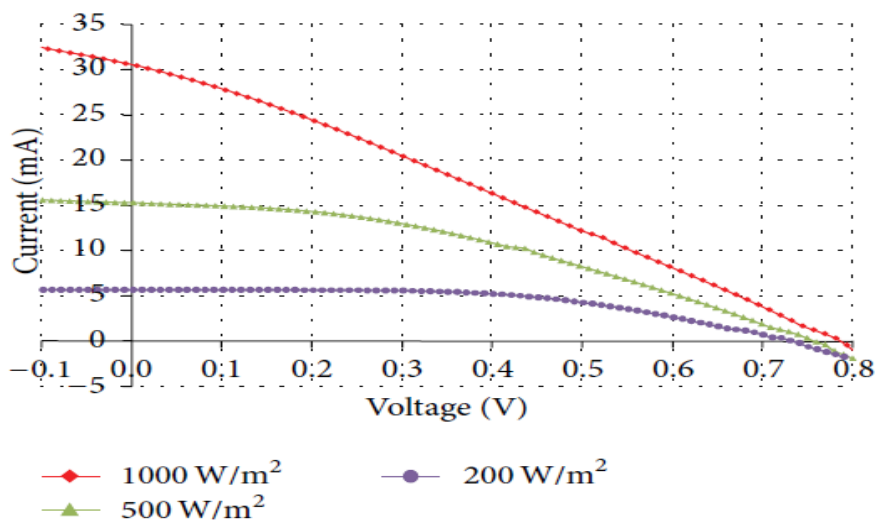
Figure 14. I-V curves of fabricated textile based PSDSSC at different irradiance level.[108]

3.2. Textile-based organic PV (OPV) PSSCs

In 2014, Seungwoo Lee et al.[109] introduced a textile-based OPV as a stitchable power source. They used an ITO coated flexible film as bottom electrode, Zinc Oxide (ZnO) as the electron transport layer, spin-coated P3T:PCBM as the bulk heterojunction photoactive layer, molybdenum trioxide (MoO_3) deposited by thermal evaporation as the hole transport layer, and finally a gold textile electrode placed as the top electrode by physical lamination onto the MoO_3 layer. The fabricated solar cell was integrated into a textile providing a PCE of 1.79% for the textile-based solar cell, and 2.97% for the reference organic solar cell with a thermally evaporated silver top electrode. Although this work demonstrated a novel idea for fabrication of a textile-based OPV device, the PCE remained low due to the purely physical connection between the gold textile electrode and the hole transport layer. In future, a cheaper method for developing the electrode connection from roll to roll production would be needed, in order to demonstrate the further viability of this approach.

William Kylberg et al.[110] introduced a flexible and transparent textile-based electrode made of woven polymer and metal fibers. The open spaces between the polymer and metal fibers were filled with a transparent polymer fabricated by immersing the woven textile in the liquid polymer and using doctor blading. Subsequently, the transparent polymer was cured and stabilized with UV light. A layer of PEDOT:PSS was coated on the prepared textile by doctor blading, and an active layer of P3HT/PCBM was spin coated on the PEDOT:PSS layer. Finally, an aluminum layer was thermally evaporated as the back contact (Figure 15). Table 9 shows the effect of the PEDOT:PSS thickness on the performance of the fabricated solar cell using the woven textile electrodes, as well as reference solar cells based on FTO coated glass. A decreasing PEDOT:PSS thickness resulted in enhanced J_{sc} values due to an increased transmittance of the transparent electrode. Bending tests for evaluating the mechanical stability of the solar fabric with bending radius 0.6 cm were carried out, and the results showed that there was no decrease in conductivity after a 100 bending cycles.
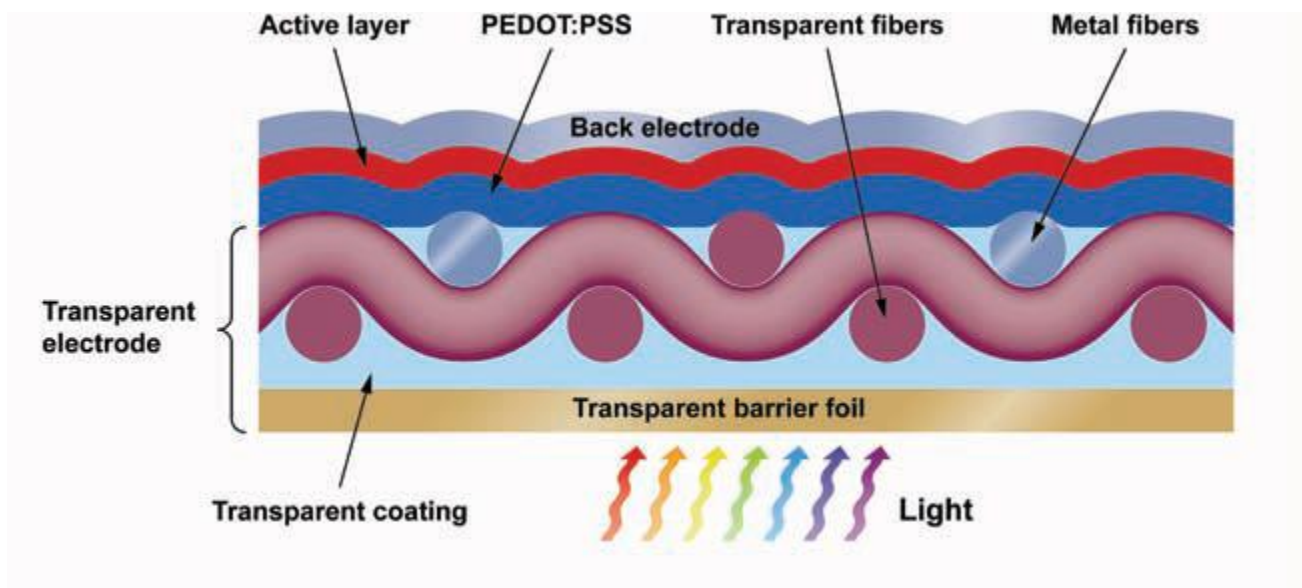

Figure 15. Cross sectional schematic view of fabricated OPV with transparent textile based top electrode.[110]

Table 9. PV performance parameters for textile based and ITO coated glass electrodes with different thickness of PEDOT:PSS.[110]

Substrate	J_{SC} (mA cm^{-2})	V_{OC} (V)	FF	PCE (%)
Fabric (1.6 μm PEDOT:PSS)	8.50	0.56	0.46	2.2 ± 0.2
Fabric (1 μm PEDOT:PSS)	11.50	0.52	0.37	2.2 ± 0.2
Glass-ITO (1.6 μm PEDOT:PSS)	9.40	0.53	0.48	2.4 ± 0.1
Glass-ITO (spin-cast PEDOT:PSS)	10.90	0.56	0.52	3.2 ± 0.1

In 2015 R. Steim et al.[111] used a conductive fabric made of poly (ethylene 2,6 naphthalate) (PEN) with Ag coated metallic woven wires as the top electrode in an organic solar cell. Aluminum-doped zinc oxide (AZO) and Ag (AZO/Ag/AZO) was coated on a polyethylene terephthalate (PET) foil from a sputtering technique. The transparent bottom electrodes had sheet resistance of 10 Ωsq^{-1}. Different layers including P3HT:PCBM, Pedot:PSS HTL, and Pedot:PSS F ET were coated on the substrate, respectively, by doctor blade technique, followed by lamination onto wet Pedot:PSS F ET films using manually applied pressure. After heating at 60ºC, the Pedot:PSS F ET strongly adhered to the fabric and the contact between the metal wires and the OPV cell was formed. Finally, the OPV was encapsulated between glasses with an epoxy based liquid adhesive. Figure 16(a) shows the schematic structure of fabricated OPV with the fabric as a top electrode. Figure 16(b) shows the J-V curves for fabricated and encapsulated solar cells, which are illuminated from both the fabric and AZO/Ag/AZO side. Results showed that for illumination from the fabric top electrode side, J_{sc} was 5mA/cm^2, the V_{oc} 0.57 V, and FF 53%, thus resulting in a PCE of 1.5%. For the illumination through the AZO/Ag/AZO bottom electrode side, a similar PCE of 1.6% was obtained, with slightly higher J_{sc} values due to the improved transparency. Although the top electrode inside this solar cell was fabric-based, the main substrate was a flexible PET sheet that is not as flexible as fabrics and textiles.
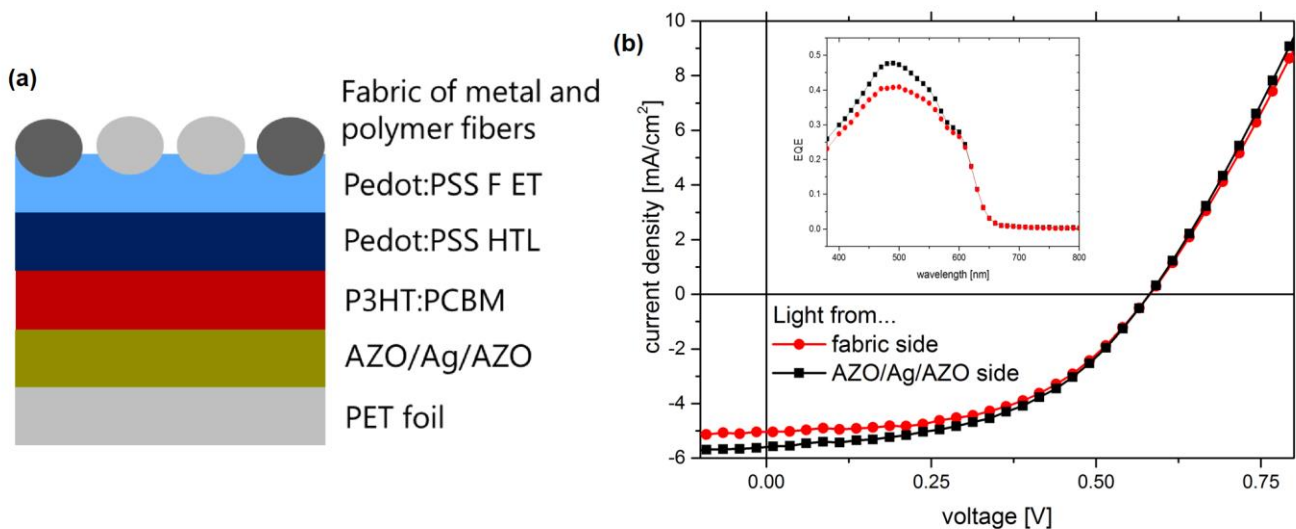

Figure 16. a) Schematic image of the structure of fabricated top electrode fabric based OPV b) J-V characteristics for the fabric based OPV with illuminated from both the fabric side and AZO/Ag/AZO side.[111]

In 2015 S. Arumugam et al.[112] fabricated an organic solar cell on a 65/35 polyester cotton woven fabric as a textile substrate. Polyurethane based interface paste was initially coated on the fabric substrate by a screen printing technique, in order to decrease the roughness and smoothening of the fabric surface. A suspension of metallic AgNW in isopropyl alcohol (IPA) was used for spray coating of AgNW as the bottom electrode. An electron transport layer of ZnO-NP with an average particle size <35 nm that had been dispersed (40 wt%) in ethanol was coated on the bottom electrode by spray coating technique. A blend of regioregular poly(3-hexylthiophene) (P3HT):indene-C60 bisadduct (ICBA), dissolved in 1,2- dichlorobenzene was used as the photoactive layer on the electron transport layer. Then a layer of poly(3,4-ethylenedioxythiophene):polystyrene sulfonate (PEDOT:PSS) dispersion in water was coated on the active layer as the hole transport layer. At last, an AgNW was coated on the hole transport layer as the top electrode (Figure 17). Figure 18 shows different SEM pictures from different aspects of the fabricated textile solar cells. Figures 19 represent J-V curves of the fabricated textile solar cells and the same PV structure on a glass substrate developed by the spray coating technique. As shown in Table 10, the reference solar cells on glass showed an expected higher performance than the textile solar cells, partially due to uniform coverage of the PEDOT:PSS layer and the smoother surface of the P3HT:ICBA layer. However, it should be noted that the fill factors of the reference devices are quite low. The approach was innovative for the fabrication of a textile solar cell that could potentially be embedded in wearable and formable devices, however, the device efficiency needs to be further boosted. This works also highlights how the development of the bottom and top electrode is one of the main challenges in this research field.
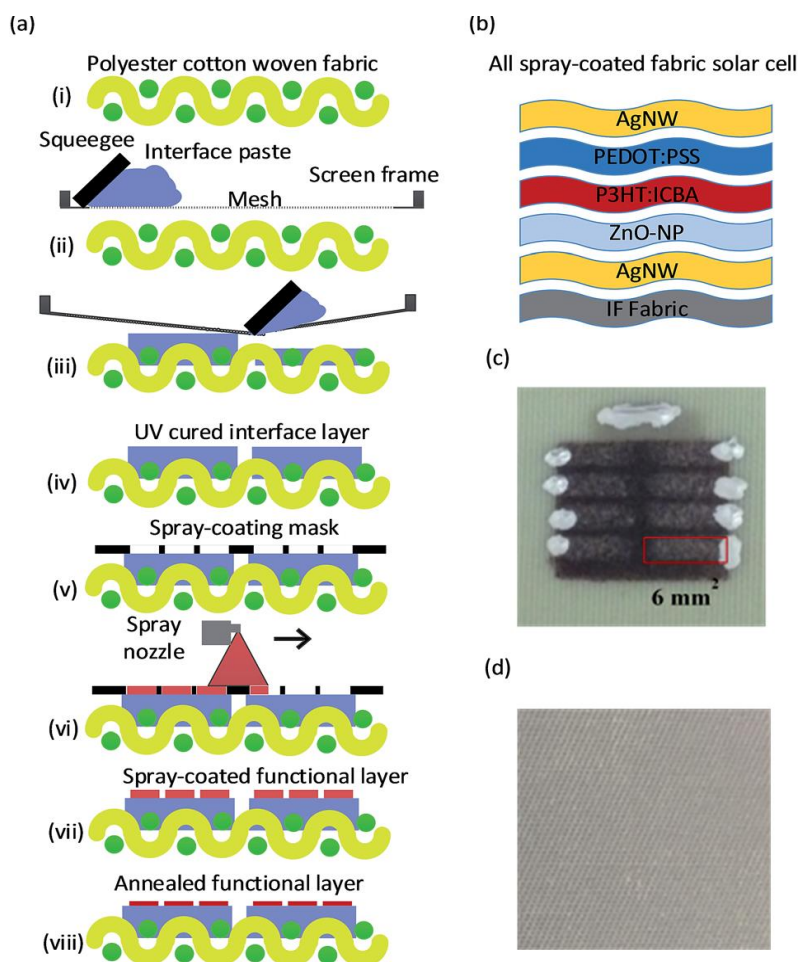
Figure 17. Schematic illustration of a) fabrication process of OPV textile based b) cross sectional view of different PV layers c) image of the fabricated OPV from the front side d) image of the fabricated OPV from the back side.[112]
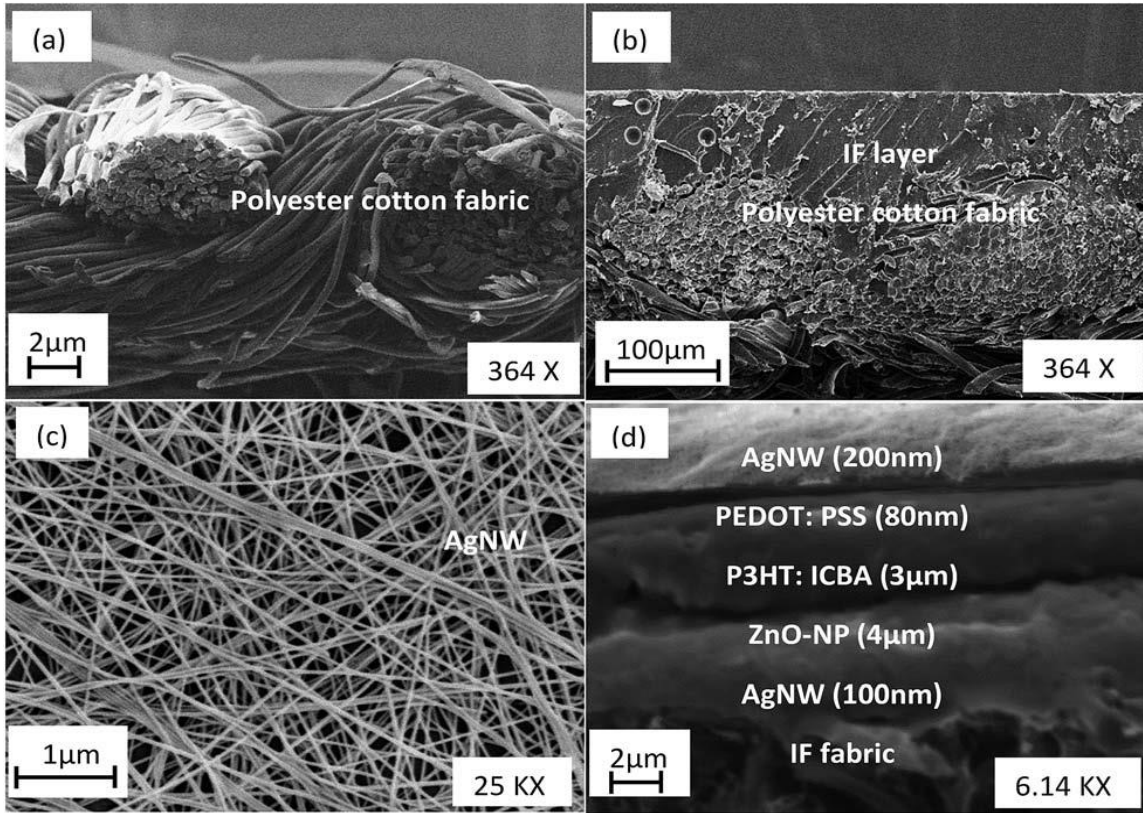
Figure 18. a) cross section SEM image of woven Polyester (65)/Cotton (35) fabric substrate b) SEM image of the coated interface layer on the fabric c) FE-SEM image of the spray coated AGNW on the fabric substrate as the bottom electrode d) SEM image (cross section view) of different PV layers.[112]
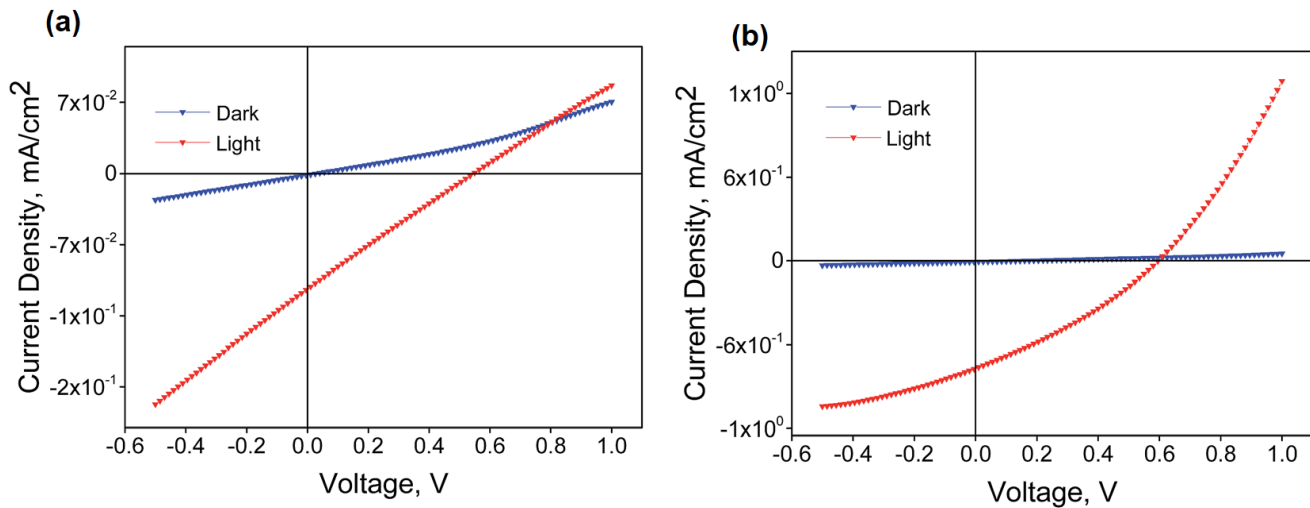
Figure 19. J-V curves of the OPV devices fabricated by spray coating technique on a) fabric substrate (type 1) b) glass substrate (type 2).[112]

Table 10. PV parameters of fabricated OPV on fabric and glass substrates.[112]

Devices	Device structure	J_{SC} (mA cm^{-2})	V_{OC} (V)	FF	PCE (%)
Type 1	IF fabric/AgNW/ZnO-NP/P3HT:ICBA/PEDOT:PSS/AgNW	0.11	0.55	0.24	0.01
Type 2	Glass/AgNW/ZnO-NP/P3HT:ICBA/PEDOT:PSS/AgNW	0.76	0.61	0.30	0.14
Type 3	IF fabric/pressed AgNW/ZnO-NP/P3HT:ICBA/PEDOT:PSS/AgNW	0.26	0.41	0.25	0.02

Recently, Yi Li et al.[113] have fabricated a textile OPV by printing and spray coating technique. They used woven 65/35 polyester cotton fabric as the textile substrate. First, they coated three interface layers on the textile substrate with overall thickness of 250 μm in order to reducing the roughness of textile substrate for achieving a smooth substrate. Then, they coated Ag electrode, ZnO layer, active layer, PEDOT:PSS layer, and Ag nanowire layer by spray coating technique. The fabricated textile OPV has V_{oc} of 0.5 V, J_{SC} of 3.44 (mA/cm^2), FF of 0.24 and PCE of 0.4%. Fabricated textile solar cells were encapsulated for protecting them from air and improving their stability. Results showed that un-encapsulated textile solar cells could not survive more than 2 days but encapsulated textile solar cells could work during 30 days with 100% PCE, during 30 to 60 days with 75% PCE, and after 60 days with less than 25% PCE.

3.3 Textile-based perovskite (PSPSCs)

In 2017, Jeun-Yan Lam et al.[114] integrated a washable and flexible perovskite solar cell on a textile. SnO$_2$ was electrodeposited on the flexible ITO coated PEN substrate as the ETL, followed by a thin layer of PCBM that was spin coated on the SnO$_2$ coated layer in order to decrease the roughness of the SnO$_2$ coated layer for improved electron transport. The perovskite layer of MAPbI$_3$ and HTL of Spiro-OMETAD were spin coated on the previous layers. Finally, a gold top electrode was thermally evaporated on the HTL layer. The fabricated solar cell was encapsulated by a 3M™ acrylic elastomer and adhered to the textile (Figure 20). The fabricated textile-based flexible perovskite solar cell was characterized immediately after development and after immersion in the water (Figure 21 and Table 11). As the J-V in Figure 21 shows, the performance of the fabricated textile solar cell was nearly stable during the water immersion cycles, demonstrating the high barrier quality in their solution. Figure 22 shows a picture of fabricated textile-based PSPSC and its application for lighting up an integrated LED inside the textile.

Although this work demonstrated the development of a textile-based perovskite solar cell with good stability properties for the application addressed, it still showed limited flexibility, as the standard perovskite cell stack was integrated directly onto the textile. Therefore, the integrated solar cell cannot be formed and folded, highlighting the remaining limitations for achieving complete device flexibility.
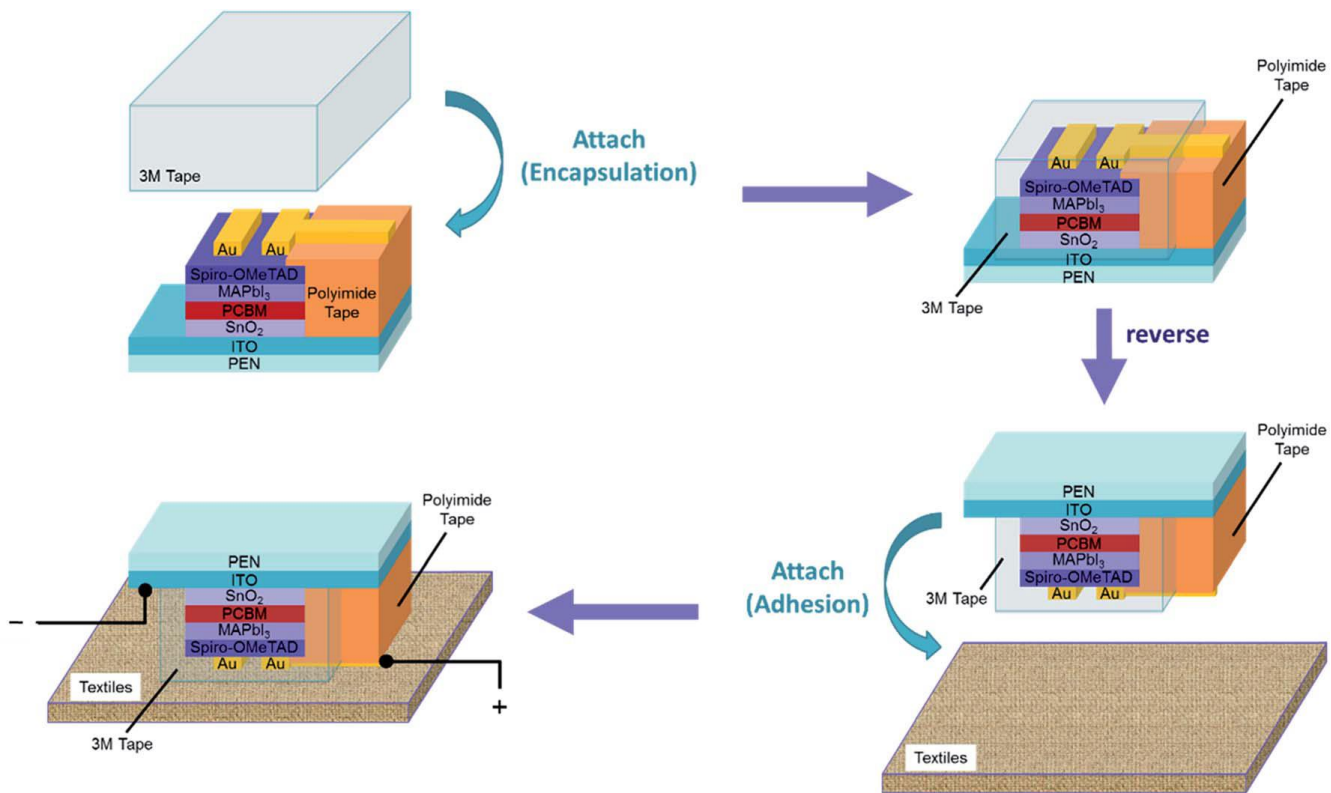
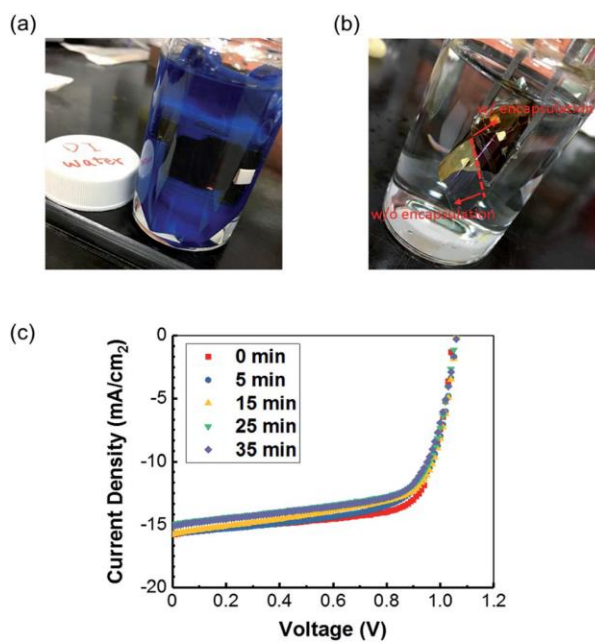Figure 20. Schematic illustration of the fabrication process of the textile-based flexible PSPSC[114]

Figure 21. a) Image of a) the textile-based PSPSC immersed in water b) fabricated textile-based PSPSC with and without encapsulation while immersing in water. c) J-V curves of the textile-based PSPSCs for different immersion times in the water.[114]
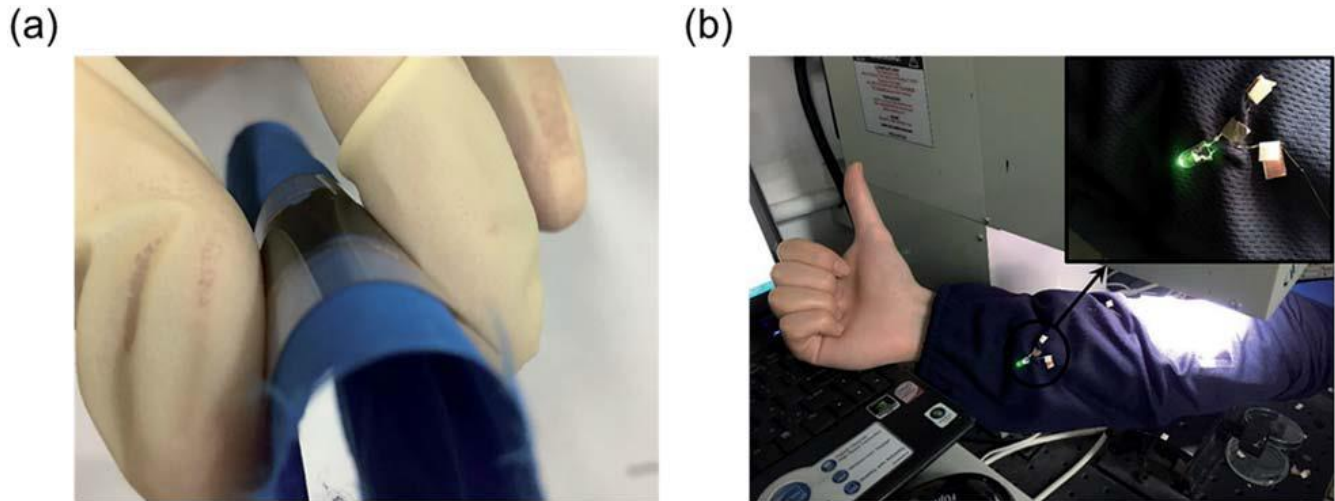
Figure 22. Image of a) fabricated flexible textile-based PSPSC b) a commercial LED lit up by the fabricated textile-based flexible PSCs under 0.8 sun illumination.[114]

Table 11. PV parameters of textile-based PSCs using SnO_2 ETL and SnO_2/PCBM ETL.[114]

Electron-transporting layer		J_{SC} (mA cm^{-2})	V_{OC} (V)	FF	PCE (%)
SnO_2 (0.8 sun)[a]	F	-13.47	1.03	0.31	5.4
SnO_2 (0.8 sun)[a]	R	-12.16	1.02	0.41	6.3
SnO_2/PCBM (0.8 sun)	F	-17.07	1.08	0.63	14.5
SnO_2/PCBM (0.8 sun)	R	-17.05	1.06	0.65	14.8
SnO_2/PCBM (1 sun)	F	-20.90	1.07	0.62	13.9
SnO_2/PCBM (1 sun)	R	-20.53	1.06	0.66	14.3

F: forward-bias sweep (-0.1 V- 1.2 V); R: reverse-bias sweep (1.2V- -0.1V). Time of electrodeposition for SnO_2: 120 s.

In 2018, Jung et al.[115] could fabricate a textile-based PSPSCs on a Polyester/satin textile substrate. They coated a thin layer of polyurethane (PU) by a paper transfer lamination method on the textile in order to have an even and smother textile substrate surface for solution-processing. After that, they coated an inverted PV architecture PEDOT:PSS by scalable printing technique as the anode instead of ITO or FTO and doctor blading 0.5 wt% single-walled carbon nanotubes (SWCNTs) in PEDOT:PSS in order to improving the conductivity /printing a low conductivity PEDOT:PSS as the Hole Transport Layer (HTL) / printing perovskite absorber layer of $CH_3NH_3PbI_3$/ printing PCBM by bar coating technique as the Electron Transport Layer (ETL). Finally, they coated with a 8nm thick transparent electrode of Ag by thermal evaporator technique. Figure 23 shows a schematic illustration for the whole of perovskite PSSCs textile-based structure and a cross-sectional SEM picture of PU coated textile substrate. The best result, which was achieved in 600 nm perovskite thickness, led to PCE of 5.17%, V_{OC} of 0.82V, J_{SC} of 12.69 mA cm^{-2}, and FF of 0.5. Table 12 shows PV parameters of fabricated perovskite textile-based with different thicknesses of perovskite layer.
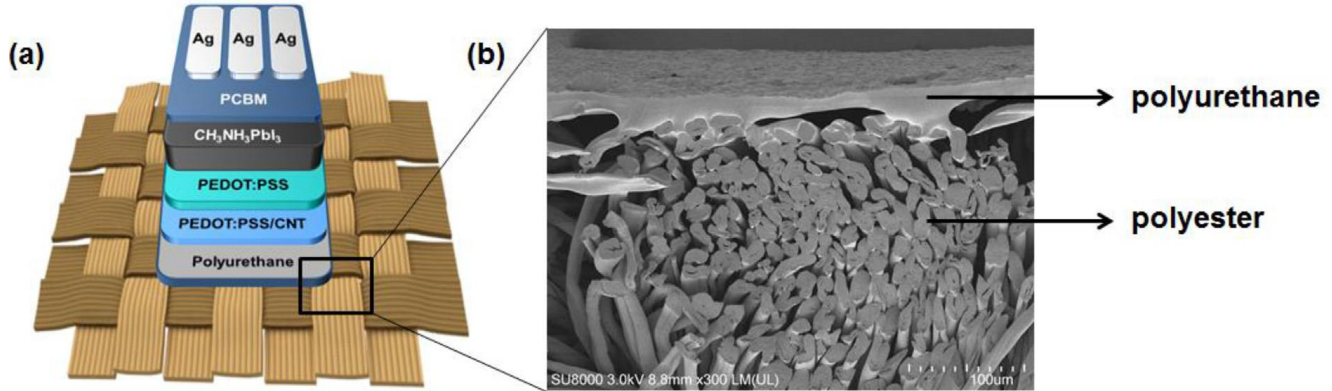
Figure 23. a) Schematic illustration of textile-based PSPSCs structure b) SEM image of the PU coated textile substrate.[115]

Table 11. PV parameters of textile-based PSPSCs with different thicknesses of perovskite layer.[115]

Thickness of perovskite [nm]	V_{OC}^b [V]	J_{SC}^b [mA cm^{-2}]	FF^b	PCE^b [%]	Integrated J_{SC} [mA cm^{-2}]
400	0.62 ± 0.02 (0.63)	7.88 ± 0.27 (8.15)	0.33 ± 0.03 (0.35)	1.72 ± 0.186 (1.75)	8.03
600	0.82 ± 0.02 (0.84)	12.18 ± 0.55 (12.69)	0.47 ± 0.02 (0.5)	4.86 ± 0.01 (5.17)	11.34
600^a	0.88 ± 0.01 (0.89)	12.44 ± 0.38 (12.91)	0.49 ± 0.03 (0.51)	5.55 (5.72)	12.28

a Solvent annealed devices.

b Values in parenthesis are the best results.

3.4. Comparison between different types of PSSCs textile-based

In most of the reported studies regarding the fabricated textile-based PSDSSCs, researchers have successfully demonstrated the development and fabrication of DSSC from a flexible textile-based counter electrode, which are important steps towards development of textile-based PVs. However, as the full DSSC is still using glass-based working electrodes in the mentioned works, the full devices were not flexible, and thus they are to be considered as part of a longer development route for textile PV devices. Fabricated textile-based OPV PSSCs are flexible enough for wearable applications, but they still perform poorly in terms of efficiencies and stability. In literature, there are fewer studies for textile-based perovskite PSSCs compared to those on other types of textile-based PSSCs, being perovskite PV a younger technology. However, the reported works demonstrate that perovskite solar cells are more promising than other solar cells for developing textile-based PSSCs due to their more compatible structure with flexible substrates, higher efficiency and stability, and at the same time easier solution-processable fabrication process.

4. Summary, challenges and outlook

In this article, the various research work done within the area of textile solar cells in recent years has been reviewed, looking into both FSSCs and textile-based PSSCs developed within the DSSC, OPV, and perovskite solar cell technologies. The high flexibility of FSSC is a unique advantage that make them capable for application in wearable power harvesting applications. Despite the promising progress on the device performance of FSSC, the fabrication of a FSSC is a cost consuming process that needs special techniques due to their three dimensions and

the cylindrical shape of the substrate. Furthermore, weaving of the FSSC is not an easy process, and special care should be taken for not introducing device damage during the weaving process. Finally, as typically only one side of the weaved FSSC will be illuminated by sunlight in wearable applications, while the back side will be dark, applications where these fiber textile solar cells can utilize their three dimensions' absorption is more reasonable than wearable applications. As an alternative, the PV materials can be developed on a textile substrate, instead of weaving FSSC into textiles as textile-based PSSCs, which is an innovative area that overcomes some of the challenges of FSSC technology. However, one challenge in PSSCs seems to be the integration of a stable and uniform planarization layer, which also leads to the relatively planarized electrodes needed for device fabrication. Evidently, device processes that can be conducted at low temperatures are needed in the final development of the textile solar cells. The fabricated textile-based PSSCs solar cell should at the end be super-flexible, light-weight, wearable, formable and foldable, which potentially hampers the barrier encapsulation requirements. Here routes that addresses highly stable active layer materials should be still considered, at least before the textile solar cells can reach a production stage. As application areas, the PSSCs textile-based solar cells could be used as the power harvesting part of smart textiles, e-textiles, and wearable electronic devices, due to their compatibility with wearable electronic applications. The PSSCs textile-based solar cells could be used in emergency situations, such as for temporary tents used in floods, earthquakes and other climate change related emergencies, where they appear ideal being light-weight and with easy installation. They could also be applied in everyday households as solar curtains for supplying the electrical energy required during the daytime. Although a few prototypes of textile-based PSSCs solar cells have been fabricated, up-scaling of these devices still needs more efforts in order to reach an optimization of the fabrication process from the prospective of the materials and the employed fabrication techniques. Encapsulation of the fabricated textile-based PSSCs solar cells still remains as another challenge which should be investigated. Here standard Roll-to-Roll (R2R) processing techniques are well suited with a variety of thin-film coating techniques available, both for solution processing and vacuum evaporation methods. It should be noted that in these device configurations employed for textile-based PSSCs solar cells, ultrahigh mechanical flexibilities are sought for, which potentially hampers the requirements on device encapsulation. Typically, these organic and hybrid solar cells are encapsulated from rigid or only partially flexible barrier layers in order to prevent the material from undertaking chemical degradation process in contact with oxygen and light, i.e. photooxidation processes. As the devices are required to be more flexible, it automatically comes along with lower barrier properties, which is a potential challenge for the stability of these devices. One route to alleviate this tradeoff could be the addition of additive assisted stabilizers added into the active layers of the devices. This has been demonstrated as a very promising route for organic solar cells, highlighting that one can reach longer device stability with lower barrier requirements[116–118]. Finally, the main key problem for making textile-based PSSCs solar cells usable in real wearable applications is their efficiency, which should be as much as high in order to supplying the electrical energy for the relevant electronic devices. At present, much efforts should still be carried out in the future to achieve this goal.

Acknowledgements

References

1. Memon AA, Patil SA, Sun KC, et al. Carbonous metallic framework of multi-walled carbon Nanotubes/Bi2S3 nanorods as heterostructure composite films for efficient quasi-solid state DSSCs. *Electrochim Acta*. 2018;283:997-1005. doi:10.1016/j.electacta.2018.04.131

2. Sahito IA, Sun KC, Lee W, Kim JP, Jeong SH. Graphene nanosheets as counter electrode with phenoxazine dye for efficient dye sensitized solar cell. *Org Electron physics, Mater Appl*. 2017;44(February):32-41. doi:10.1016/j.orgel.2017.01.035

3. Ren Y, Sun D, Cao Y, et al. A Stable Blue Photosensitizer for Color Palette of Dye-Sensitized Solar Cells Reaching 12.6% Efficiency. *J Am Chem Soc*. 2018;140(7):2405-2408. doi:10.1021/jacs.7b12348

4. Lu W, Jiang R, Yin X, Wang L. Porous N-doped-carbon coated CoSe2anchored on carbon cloth as 3D photocathode for dye-sensitized solar cell with efficiency and stability outperforming Pt. *Nano Research*. 2018:1-5.

5. Jing H, Shi Y, Qiu W, et al. Onion-like graphitic carbon covering metallic nanocrystals derived from brown coal as a stable and efficient counter electrode for dye-sensitized solar cells. *J Power Sources*. 2019;414(October 2018):495-501. doi:10.1016/j.jpowsour.2019.01.042

6. Bandara TMWJ, Ajith Desilva L, Ratnasekera JL, et al. High efficiency dye-sensitized solar cell based on a novel gel polymer electrolyte containing RbI and tetrahexylammonium iodide (Hex 4 NI) salts and multi-layered photoelectrodes of TiO 2 nanoparticles. *Renew Sustain Energy Rev*. 2019;103(December 2018):282-290. doi:10.1016/j.rser.2018.12.052

7. Huang Y, Wu H, Yu Q, et al. Single-Layer TiO2Film Composed of Mesoporous Spheres for High-Efficiency and Stable Dye-Sensitized Solar Cells. *ACS Sustain Chem Eng*. 2018;6(3):3411-3418. doi:10.1021/acssuschemeng.7b03626

8. Zhang W, Wu Y, Bahng HW, et al. Comprehensive control of voltage loss enables 11.7% efficient solid-state dye-sensitized solar cells. *Energy Environ Sci*. 2018;11(7):1779-1787. doi:10.1039/c8ee00661j

9. Wang P, Yang L, Wu H, et al. Stable and Efficient Organic Dye-Sensitized Solar Cell Based on Ionic Liquid Electrolyte. *Joule*. 2018;2(10):2145-2153. doi:10.1016/j.joule.2018.07.023

10. Xu B, Tian L, Etman AS, Sun J, Tian H. Solution-processed nanoporous NiO-dye-ZnO photocathodes: Toward efficient and stable solid-state p-type dye-sensitized solar cells and dye-sensitized photoelectrosynthesis cells. *Nano Energy*. 2019;55:59-64. doi:10.1016/j.nanoen.2018.10.054

11. Rafique S, Abdullah SM, Sulaiman K, Iwamoto M. Fundamentals of bulk heterojunction organic solar cells: An overview of stability/degradation issues and strategies for improvement. *Renew Sustain Energy Rev*. 2018;84(December 2017):43-53. doi:10.1016/j.rser.2017.12.008

12. Ali A, Kazici M, Bozar S, et al. Laminated Carbon Nanotubes for the Facile Fabrication of Cost-Effective Polymer Solar Cells. *ACS Appl Energy Mater*. 2018;1(3):1226-1232. doi:10.1021/acsaem.7b00345

13. Li S, Zhan L, Liu F, et al. An Unfused-Core-Based Nonfullerene Acceptor Enables High-Efficiency Organic Solar Cells with Excellent Morphological Stability at High Temperatures. *Adv Mater*. 2018;30(6):1-8. doi:10.1002/adma.201705208

14. Du X, Heumueller T, Gruber W, et al. Efficient Polymer Solar Cells Based on Non-fullerene Acceptors with Potential Device Lifetime Approaching 10 Years. *Joule*. 2018:1-12. doi:10.1016/j.joule.2018.09.001

15. Patil BR, Mirsafaei M, Cielecki PP, et al. ITO with embedded silver grids as transparent conductive electrodes for large area organic solar cells. *Nanotechnology*. 2017;28(40). doi:10.1088/1361-6528/aa820a

16. Ciammaruchi L, Oliveira R, Charas A, et al. Stability of organic solar cells with PCDTBT donor polymer: An interlaboratory study. *J Mater Res*. 2018;33(13):1909-1924. doi:10.1557/jmr.2018.163

17. Ahmadpour M, Fernandes Cauduro AL, Méthivier C, et al. Crystalline Molybdenum Oxide Layers as Efficient and Stable Hole Contacts in Organic Photovoltaic Devices. *ACS Appl Energy Mater*. 2019:acsaem.8b01452. doi:10.1021/acsaem.8b01452

18. An Q, Zhang F, Gao W, et al. High-efficiency and air stable fullerene-free ternary organic solar cells. *Nano Energy*. 2018;45:177-183. doi:10.1016/j.nanoen.2017.12.050

19. Ye L, Xiong Y, Zhang Q, et al. Surpassing 10% Efficiency Benchmark for Nonfullerene Organic Solar Cells by Scalable Coating in Air from Single Nonhalogenated Solvent. *Adv Mater*. 2018;30(8). doi:10.1002/adma.201705485

20. Lee HKH, Durrant JR, Li Z, Tsoi WC. Stability study of thermal cycling on organic solar cells. *J Mater Res*. 2018;33(13):1902-1908. doi:10.1557/jmr.2018.167

21. Gasparini N, Wadsworth A, Moser M, Baran D, McCulloch I, Brabec CJ. The Physics of Small Molecule Acceptors for Efficient and Stable Bulk Heterojunction Solar Cells. *Adv Energy Mater*. 2018;8(12):1-15. doi:10.1002/aenm.201703298

22. Upama MB, Elumalai NK, Mahmud MA, et al. Effect of annealing dependent blend morphology and dielectric properties on the performance and stability of non-fullerene organic solar cells. *Sol Energy Mater Sol Cells*. 2018;176(November 2017):109-118. doi:10.1016/j.solmat.2017.11.027

23. Wang D, Elumalai NK, Mahmud MA, et al. MoS2 incorporated hybrid hole transport layer for high performance and stable perovskite solar cells. *Synth Met*. 2018;246(January 2019):195-203. doi:10.1016/j.synthmet.2018.10.012

24. Li X, Xue Z, Luo D, et al. A stable lead halide perovskite nanocrystals protected by PMMA. *Sci China Mater*. 2018;61(3):363-370. doi:10.1007/s40843-017-9148-7

25. Mahmood K, Mehran MT, Rehman F, Zafar MS, Ahmad SW, Song RH. Electrosprayed Polymer-Hybridized Multidoped ZnO Mesoscopic Nanocrystals Yield Highly Efficient and Stable Perovskite Solar Cells. *ACS Omega*. 2018;3(8):9648-9657. doi:10.1021/acsomega.8b01412

26. Mingorance A, Xie H, Kim H, et al. Interfacial Engineering of Metal Oxides for Highly Stable Halide Perovskite Solar Cells. 2018;1800367:1-10. doi:10.1002/admi.201800367

27. Mahmud MA, Elumalai NK, Upama MB, et al. A high performance and low-cost hole transporting layer for efficient and stable perovskite solar cells. *Phys Chem Chem Phys*. 2017;19(31):21033-21045. doi:10.1039/c7cp03551a

28. Aineh N, Castro-Méndez AF, Rodriguez-Cantó PJ, et al. Optical Optimization of the TiO2Mesoporous Layer in Perovskite Solar Cells by the Addition of SiO2Nanoparticles. *ACS Omega*. 2018;3(8):9798-9804. doi:10.1021/acsomega.8b01119

29. Jeon NJ, Noh JH, Kim YC, Yang WS, Ryu S, Seok S Il. Solvent engineering for high-performance inorganic-organic hybrid perovskite solar cells. *Nat Mater*. 2014;13(9):897-903. doi:10.1038/nmat4014

30. Islavath N, Lingamallu G. The performance enhancement of HTM-free ZnO nanowire-based perovskite solar cells via low-temperature TiCl4treatment. *Sol Energy*. 2018;170(October):158-163.

doi:10.1016/j.solener.2018.05.050

31. Fakharuddin A, Seybold M, Agresti A, et al. Perovskite-polymer blends influencing microstructure, non-radiative recombination pathways and photovoltaic performance of perovskite solar cells. *ACS Appl Mater Interfaces*. 2018:acsami.8b18200. doi:10.1021/acsami.8b18200

32. Saygili Y, Turren-Cruz SH, Olthof S, et al. Planar Perovskite Solar Cells with High Open-Circuit Voltage Containing a Supramolecular Iron Complex as Hole Transport Material Dopant. *ChemPhysChem*. 2018;19(11):1363-1370. doi:10.1002/cphc.201800032

33. Zhang F, Zhao X, Yi C, et al. Dopant-free star-shaped hole-transport materials for efficient and stable perovskite solar cells. *Dye Pigment*. 2017;136:273-277. doi:10.1016/j.dyepig.2016.08.002

34. Qin J, Zhang Z, Shi W, Liu Y, Gao H, Mao Y. The optimum titanium precursor of fabricating TiO2compact layer for perovskite solar cells. *Nanoscale Res Lett*. 2017;12(1). doi:10.1186/s11671-017-2418-9

35. Shirazi M, Toroghinejad MR, Sabet Dariani R, Hosseinnejad MT. Fabrication of hole-conductor-free perovskite solar cells based on Al doped ZnO and low-cost carbon electrode. *J Mater Sci Mater Electron*. 2018;29(12):10092-10101. doi:10.1007/s10854-018-9054-8

36. Ngo TT, Barea EM, Tena-Zaera R, Mora-Seró I. Spray-Pyrolyzed ZnO as Electron Selective Contact for Long Term Stable Planar CH3NH3PbI3 Perovskite Solar Cells. *ACS Appl Energy Mater*. 2018;(August):acsaem.8b00733. doi:10.1021/acsaem.8b00733

37. Mei A, Li X, Liu L, et al. A hole-conductor-free, fully printable mesoscopic perovskite solar cell with high stability. *Science (80-)*. 2014;345(6194):295-298. doi:10.1126/science.1254763

38. Konstantakou M, Perganti D, Falaras P, Stergiopoulos T. Anti-Solvent Crystallization Strategies for Highly Efficient Perovskite Solar Cells. 2017:1-21. doi:10.3390/cryst7100291

39. Chandrasekhar PS, Dubey A, Reza KM, et al. Higher efficiency perovskite solar cells using 2 core–shell nanoparticles. *Sustain Energy Fuels*. 2018:2260-2267. doi:10.1039/C7SE00472A

40. Cheng J, Zhang H, Zhang S, et al. Highly efficient planar perovskite solar cells achieved by simultaneous defect engineering and formation kinetic control. *J Mater Chem A*. 2018;(November). doi:10.1039/C8TA08819E

41. Hua Y, Liu P, Li Y, Sun L, Kloo L. Composite Hole-Transport Materials Based on a Metal-Organic Copper Complex and Spiro-OMeTAD for Efficient Perovskite Solar Cells. 2018;1700073:1-7. doi:10.1002/solr.201700073

42. Khenkin M V., Anoop KM, Visoly-Fisher I, et al. Reconsidering figures of merit for performance and stability of perovskite photovoltaics. *Energy Environ Sci*. 2018;11(4):739-743. doi:10.1039/c7ee02956j

43. Li L, Zhang S, Yang Z, Berthold EES, Chen W. Recent advances of flexible perovskite solar cells. *J Energy Chem*. 2018;(April). doi:10.1016/j.jechem.2018.01.003

44. Zhang Z, Lv R, Jia Y, Gan X, Zhu H, Kang F. All-Carbon Electrodes for Flexible Solar Cells. *Appl Sci*. 2018;8(2):152. doi:10.3390/app8020152

45. Heo JH, Lee MH, Han HJ, Patil BR, Yu JS, Im SH. Highly efficient low temperature solution processable planar type CH3NH3PbI3perovskite flexible solar cells. *J Mater Chem A*. 2016;4(5):1572-1578. doi:10.1039/c5ta09520d

46. Heo JH, Shin DH, Jang MH, Lee ML, Kang MG, Im SH. Highly flexible, high-performance perovskite solar cells with adhesion promoted AuCl3-doped graphene electrodes. *J Mater Chem A*.

2017;5(40):21146-21152. doi:10.1039/c7ta06465a

47. Heo JH, Shin DH, Song DH, Kim DH, Lee SJ, Im SH. Super-flexible bis(trifluoromethanesulfonyl)-amide doped graphene transparent conductive electrodes for photo-stable perovskite solar cells. *J Mater Chem A*. 2018;6(18):8251-8258. doi:10.1039/c8ta02672f

48. Hu Y, Zhang S, Shu T, et al. Highly efficient flexible solar cells based on a room-temperature processed inorganic perovskite. *J Mater Chem A*. 2018;6(41):20365-20373. doi:10.1039/c8ta06719h

49. Kamaraki C, Zachariadis A, Kapnopoulos C, et al. Efficient flexible printed perovskite solar cells based on lead acetate precursor. *Sol Energy*. 2018;176(September):406-411. doi:10.1016/j.solener.2018.10.055

50. Khadem M, Park TL, Penkov O V., Kim DE. Highly transparent micro-patterned protective coatings on polyethylene terephthalate for flexible solar cell applications. *Sol Energy*. 2018;171(April):629-637. doi:10.1016/j.solener.2018.07.023

51. Kim JH, Seok HJ, Seo HJ, et al. *Flexible ITO Films with Atomically Flat Surfaces for High Performance Flexible Perovskite Solar Cells*. Vol 10.; 2018. doi:10.1039/c8nr06586a

52. Li G, Sheng L, Li T, Hu J, Li P, Wang K. Engineering flexible dye-sensitized solar cells for portable electronics. *Sol Energy*. 2019;177(November 2018):80-98. doi:10.1016/j.solener.2018.11.017

53. Fu X, Xu L, Li J, Sun X, Peng H. Flexible solar cells based on carbon nanomaterials. *Carbon N Y*. 2018;139:1063-1073. doi:10.1016/j.carbon.2018.08.017

54. Yoon J, Sung H, Lee G, et al. Superflexible, high-efficiency perovskite solar cells utilizing graphene electrodes: towards future foldable power sources. *Energy Environ Sci*. 2017;10(1):337-345. doi:10.1039/C6EE02650H

55. Popoola IK, Gondal MA, Qahtan TF. Recent progress in flexible perovskite solar cells: Materials, mechanical tolerance and stability. *Renew Sustain Energy Rev*. 2018;82:3127-3151. doi:10.1016/J.RSER.2017.10.028

56. Lund PD, Halme J, Hashmi G, Asghar I, Miettunen K. Application of dye-sensitized and perovskite solar cells on flexible substrates. *Flex Print Electron*. 2018;3(1):13002. doi:10.1088/2058-8585/aaabc9

57. Lam JY, Chen JY, Tsai PC, et al. A stable, efficient textile-based flexible perovskite solar cell with improved washable and deployable capabilities for wearable device applications. *RSC Adv*. 2017;7(86):54361-54368. doi:10.1039/c7ra10321b

58. Jayenta Singh T, Singh S, Masiul Islam S, Get R, Mahala P, Jolson Singh K. Flexible organic solar cells with graphene/PEDOT:PSS Schottky junction on PET substrates. *Optik (Stuttg)*. 2019;181:984-992. doi:10.1016/j.ijleo.2018.12.179

59. Zhang X, Öberg VA, Du J, Liu J, Johansson EMJ. Extremely lightweight and ultra-flexible infrared light-converting quantum dot solar cells with high power-per-weight output using a solution-processed bending durable silver nanowire-based electrode. *Energy Environ Sci*. 2018;11(2):354-364. doi:10.1039/c7ee02772a

60. Di Giacomo F, Fakharuddin A, Jose R, Brown TM. Progress, challenges and perspectives in flexible perovskite solar cells. *Energy Environ Sci*. 2016;9(10):3007-3035. doi:10.1039/c6ee01137c

61. Guterman S, Wen X, Gudavalli G, et al. Optimized flexible cover films for improved conversion efficiency in thin film flexible solar cells. *Opt Mater (Amst)*. 2018;79(January):243-246. doi:10.1016/j.optmat.2018.03.034

62. Wu Z, Li P, Zhang Y, Zheng Z. Flexible and Stretchable Perovskite Solar Cells: Device Design and

Development Methods. *Small Methods*. 2018;2(7):1800031. doi:10.1002/smtd.201800031

63.   Lv T, Yao Y, Li N, Chen T. Wearable fiber-shaped energy conversion and storage devices based on aligned carbon nanotubes. *Nano Today*. 2016;11(5):644-660. doi:10.1016/j.nantod.2016.08.010

64.   Stoppa M, Chiolerio A. Wearable electronics and smart textiles: A critical review. *Sensors (Switzerland)*. 2014;14(7):11957-11992. doi:10.3390/s140711957

65.   Sahito IA, Khatri A. Smart and Electronic Textiles. 2017;(January).

66.   Peng M, Dong B, Zou D. Three dimensional photovoltaic fibers for wearable energy harvesting and conversion. *J Energy Chem*. 2018;27(3):611-621. doi:10.1016/j.jechem.2018.01.008

67.   Chen T, Qiu L, Yang Z, Peng H. Novel solar cells in a wire format. *Chem Soc Rev*. 2013;42(12):5031-5041. doi:10.1039/c3cs35465b

68.   J. Varma S, Sambath Kumar K, Seal S, Rajaraman S, Thomas J. Fiber-Type Solar Cells, Nanogenerators, Batteries, and Supercapacitors for Wearable Applications. *Adv Sci*. 2018;5(9). doi:10.1002/advs.201800340

69.   Zou D, Wang D, Chu Z, Lv Z, Fan X. Fiber-shaped flexible solar cells. *Coord Chem Rev*. 2010;254(9-10):1169-1178. doi:10.1016/j.ccr.2010.02.012

70.   Pu X, Song W, Liu M, et al. Wearable Power-Textiles by Integrating Fabric Triboelectric Nanogenerators and Fiber-Shaped Dye-Sensitized Solar Cells. *Adv Energy Mater*. 2016;6(20). doi:10.1002/aenm.201601048

71.   Liu G, Wang M, Wang H, et al. Hierarchically structured photoanode with enhanced charge collection and light harvesting abilities for fiber-shaped dye-sensitized solar cells. *Nano Energy*. 2018;49:95-102. doi:10.1016/j.nanoen.2018.04.037

72.   Chen T, Qiu L, Yang Z, et al. An integrated "energy wire" for both photoelectric conversion and energy storage. *Angew Chemie - Int Ed*. 2012;51(48):11977-11980. doi:10.1002/anie.201207023

73.   Peng M, Dong B, Cai X, et al. Organic dye-sensitized photovoltaic fibers. *Sol Energy*. 2017;150:161-165. doi:10.1016/j.solener.2017.04.007

74.   Toivola M, Ferenets M, Lund P, Harlin A. Photovoltaic fiber. *Thin Solid Films*. 2009;517(8):2799-2802. doi:10.1016/j.tsf.2008.11.057

75.   Peng M, Zou D. Flexible fiber/wire-shaped solar cells in progress: Properties, materials, and designs. *J Mater Chem A*. 2015;3(41):20435-20458. doi:10.1039/c5ta03731j

76.   Yang Z, Deng J, Sun X, Li H, Peng H. Stretchable, wearable dye-sensitized solar cells. *Adv Mater*. 2014;26(17):2643-2647. doi:10.1002/adma.201400152

77.   Li H, Guo J, Sun H, Fang X, Wang D, Peng H. Stable Hydrophobic Ionic Liquid Gel Electrolyte for Stretchable Fiber-Shaped Dye-Sensitized Solar Cell. *ChemNanoMat*. 2015;1(6):399-402. doi:10.1002/cnma.201500093

78.   Chen L, Zhou Y, Dai H, Yu T, Liu J, Zou Z. One-step growth of CoNi2S4 nanoribbons on carbon fibers as platinum-free counter electrodes for fiber-shaped dye-sensitized solar cells with high performance: Polymorph-dependent conversion efficiency. *Nano Energy*. 2015;11:697-703. doi:10.1016/j.nanoen.2014.11.047

79.   Song W, Wang H, Liu G, Peng M, Zou D. Improving the photovoltaic performance and flexibility of fiber-shaped dye-sensitized solar cells with atomic layer deposition. *Nano Energy*. 2016;19:1-7.

doi:10.1016/j.nanoen.2015.11.006

80. Wen Z, Yeh MH, Guo H, et al. Self-powered textile for Wearable electronics by hybridizing fiber-shaped nanogenerators, solar cells, and supercapacitors. *Sci Adv*. 2016;2(10). doi:10.1126/sciadv.1600097

81. Liu G, Wang H, Wang M, et al. Study on a stretchable, fiber-shaped, and TiO2nanowire array-based dye-sensitized solar cell with electrochemical impedance spectroscopy method. *Electrochim Acta*. 2018;267:34-40. doi:10.1016/j.electacta.2018.02.075

82. Li Z, Zhou Y, Yang Y, Dai H. Electrophoretic deposition of graphene-TiO2hierarchical spheres onto Ti thread for flexible fiber-shaped dye-sensitized solar cells. *Mater Des*. 2016;105:352-358. doi:10.1016/j.matdes.2016.05.060

83. Peng M, Yan K, Hu H, Shen D, Song W, Zou D. Efficient fiber shaped zinc bromide batteries and dye sensitized solar cells for flexible power sources. *J Mater Chem C*. 2015;3(10):2157-2165. doi:10.1039/c4tc02997f

84. Fu X, Sun H, Xie S, et al. A fiber-shaped solar cell showing a record power conversion efficiency of 10%. *J Mater Chem A*. 2018;6(1):45-51. doi:10.1039/c7ta08637g

85. Zhang Z, Yang Z, Deng J, Zhang Y, Guan G, Peng H. Stretchable polymer solar cell fibers. *Small*. 2015;11(6):675-680. doi:10.1002/smll.201400874

86. Greulich-Weber S, Zöller M, Friedel B. Textile Solar Cells Based on SiC Microwires. *Mater Sci Forum*. 2009;615-617(January):239-242. doi:10.4028/www.scientific.net/MSF.615-617.239

87. Ebner M, Schennach R, Chien H-T, Mayrhofer C, Zankel A, Friedel B. Regenerated cellulose fiber solar cell. *Flex Print Electron*. 2017;2(1):014002. doi:10.1088/2058-8585/aa5707

88. Zhang Z, Yang Z, Wu Z, et al. Weaving efficient polymer solar cell wires into flexible power textiles. *Adv Energy Mater*. 2014;4(11):1-6. doi:10.1002/aenm.201301750

89. Qiu L, Deng J, Lu X, Yang Z, Peng H. Integrating Perovskite Solar Cells into a Flexible Fiber. *Angew Chemie Int Ed*. 2014;53(39):10425-10428. doi:10.1002/anie.201404973

90. Lee M, Ko Y, Jun Y. Efficient fiber-shaped perovskite photovoltaics using silver nanowires as top electrode. *J Mater Chem A*. 2015;3:19310-19313. doi:10.1039/C5TA02779A

91. Li R, Xiang X, Tong X, Zou J, Li Q. Wearable Double-Twisted Fibrous Perovskite Solar Cell. *Adv Mater*. 2015;27(25):3831-3835. doi:10.1002/adma.201501333

92. He S, Qiu L, Fang X, et al. Radically grown obelisk-like ZnO arrays for perovskite solar cell fibers and fabrics through a mild solution process. *J Mater Chem A*. 2015;3(18):9406-9410. doi:10.1039/C5TA01532D

93. Hu H, Yan K, Peng M, et al. Fiber-shaped perovskite solar cells with 5.3% efficiency. *J Mater Chem A*. 2016;4(10):3901-3906. doi:10.1039/c5ta09280a

94. Qiu L, He S, Yang J, Deng J, Peng H. Fiber-Shaped Perovskite Solar Cells with High Power Conversion Efficiency. *Small*. 2016;12(18):2419-2424. doi:10.1002/smll.201600326

95. Qiu L, He S, Yang J, et al. An All-Solid-State Fiber-Type Solar Cell Achieving 9.49% Efficiency. *J Mater Chem A*. 2016:10105-10109. doi:10.1039/C6TA03263J

96. Wang X, Kulkarni SA, Li Z, et al. Wire-shaped perovskite solar cell based on TiO2nanotubes. *Nanotechnology*. 2016;27(20). doi:10.1088/0957-4484/27/20/20LT01

97. Hu H, Dong B, Chen B, Gao X, Zou D. High performance fiber-shaped perovskite solar cells based on lead acetate precursor. *Sustain Energy Fuels*. 2017. doi:10.1039/C7SE00462A

98. Sun H, You X, Deng J, et al. Novel graphene/carbon nanotube composite fibers for efficient wire-shaped miniature energy devices. *Adv Mater*. 2014;26(18):2868-2873. doi:10.1002/adma.201305188

99. Deng J, Qiu L, Lu X, et al. Elastic perovskite solar cells. *J Mater Chem A*. 2015;3(42):21070-21076. doi:10.1039/c5ta06156c

100. Zhang S, Fang Y, Zou D, Zhang C, Cai X. Application of carbon fibers to flexible, miniaturized wire/fiber-shaped energy conversion and storage devices. *J Mater Chem A*. 2016;5(6):2444-2459. doi:10.1039/c6ta07868k

101. Qiu L, He S, Yang J, et al. An all-solid-state fiber-type solar cell achieving 9.49% efficiency. *J Mater Chem A*. 2016;4(26):10105-10109. doi:10.1039/c6ta03263j

102. Xu J, Li M, Wu L, et al. A flexible polypyrrole-coated fabric counter electrode for dye-sensitized solar cells. *J Power Sources*. 2014;257(July):230-236. doi:10.1016/j.jpowsour.2014.01.123

103. Arbab AA, Sun KC, Sahito IA, Qadir MB, Jeong SH. Multiwalled carbon nanotube coated polyester fabric as textile based flexible counter electrode for dye sensitized solar cell. *Phys Chem Chem Phys*. 2015;17(19):12957-12969. doi:10.1039/C5CP00818B

104. Sahito IA, Sun KC, Arbab AA, Qadir MB, Choi YS, Jeong SH. Flexible and conductive cotton fabric counter electrode coated with graphene nanosheets for high efficiency dye sensitized solar cell. *J Power Sources*. 2016;319(April):90-98. doi:10.1016/j.jpowsour.2016.04.025

105. Arbab AA, Sun KC, Sahito IA, Memon AA, Choi YS, Jeong SH. Fabrication of textile fabric counter electrodes using activated charcoal doped multi walled carbon nanotube hybrids for dye sensitized solar cells. *J Mater Chem A*. 2016;4(4):1495-1505. doi:10.1039/C5TA08858E

106. Memon AA, Arbab AA, Sahito IA, Sun KC, Mengal N, Jeong SH. Synthesis of highly photo-catalytic and electro-catalytic active textile structured carbon electrode and its application in DSSCs. *Sol Energy*. 2017;150(April):521-531. doi:10.1016/j.solener.2017.04.052

107. Yun MJ, Cha SI, Seo SH, Kim HS, Lee DY. Insertion of Dye-Sensitized Solar Cells in Textiles using a Conventional Weaving Process. *Sci Rep*. 2015;5:1-8. doi:10.1038/srep11022

108. Opwis K, Gutmann JS, Lagunas Alonso AR, et al. Preparation of a Textile-Based Dye-Sensitized Solar Cell. *Int J Photoenergy*. 2016;2016(January). doi:10.1155/2016/3796074

109. Lee S, Lee Y, Park J, Choi D. Stitchable organic photovoltaic cells with textile electrodes. *Nano Energy*. 2014;9:88-93. doi:10.1016/j.nanoen.2014.06.017

110. Kylberg W, De Castro FA, Chabrecek P, et al. Woven electrodes for flexible organic photovoltaic cells. *Adv Mater*. 2011;23(8):1015-1019. doi:10.1002/adma.201003391

111. Steim R, Chabrecek P, Sonderegger U, et al. Laminated fabric as top electrode for organic photovoltaics. *Appl Phys Lett*. 2015;106(19). doi:10.1063/1.4919940

112. Arumugam S, Li Y, Senthilarasu S, et al. Fully spray-coated organic solar cells on woven polyester cotton fabrics for wearable energy harvesting applications. *J Mater Chem A*. 2016;4(15):5561-5568. doi:10.1039/c5ta03389f

113. Li Y, Arumugam S, Krishnan C, Charlton MDB, Beeby SP. Encapsulated Textile Organic Solar Cells Fabricated by Spray Coating. *ChemistrySelect*. 2019;4(1):407-412. doi:10.1002/slct.201803929

114. Lam J-Y, Chen J-Y, Tsai P-C, et al. A stable, efficient textile-based flexible perovskite solar cell with improved washable and deployable capabilities for wearable device applications. *RSC Adv*. 2017;7(86):54361-54368. doi:10.1039/C7RA10321B

115. Jung JW, Bae JH, Ko JH, Lee W. Fully solution-processed indium tin oxide-free textile-based flexible solar cells made of an organic–inorganic perovskite absorber: Toward a wearable power source. *J Power Sources*. 2018;402(August):327-332. doi:10.1016/j.jpowsour.2018.09.038

116. Turkovic V, Engmann S, Tsierkezos N, et al. Long-term stabilization of organic solar cells using UV absorbers. *J Phys D Appl Phys*. 2016;49(12). doi:10.1088/0022-3727/49/12/125604

117. Turkovic DV. Long-Term Stabilization of Organic Solar Cells Using Additives. 2014;(April). doi:10.1016/j.clinph.2009.12.037

118. Salvador M, Gasparini N, Perea JD, et al. Suppressing photooxidation of conjugated polymers and their blends with fullerenes through nickel chelates. *Energy Environ Sci*. 2017;10(9):2005-2016. doi:10.1039/c7ee01403a